(12) INTERNATIONAL APPLICATION PUBLISHED UNDER THE PATENT COOPERATION TREATY (PCT)

(19) World Intellectual Property Organization
International Bureau

(43) International Publication Date
04 January 2024 (04.01.2024)

WIPO | PCT

(10) International Publication Number
WO 2024/003537 A1

(51) International Patent Classification:
*A61N 1/36* (2006.01) *A61B 5/24* (2021.01)
*A61N 1/02* (2006.01) *A61N 1/05* (2006.01)

(21) International Application Number:
PCT/GB2023/051670

(22) International Filing Date:
27 June 2023 (27.06.2023)

(25) Filing Language: English

(26) Publication Language: English

(30) Priority Data:
2209708.3 01 July 2022 (01.07.2022) GB

(71) Applicant: **OXFORD UNIVERSITY INNOVATION LIMITED** [GB/GB]; Buxton Court, 3 West Way, Oxford OX2 0JB (GB).

(72) Inventors: **DUCHET, Benoit**; University of Oxford, MRC Brain Network Dynamics Unit, Mansfield Road, Oxford OX1 3TH (GB). **DENISON, Timothy**; University of Oxford, Institute of Biomedical Engineering, Old Road Campus Research Building, Oxford OX3 7DQ (GB). **BOGACZ, Rafal**; University of Oxford, MRC Brain Network Dynamics Unit, Mansfield Road, Oxford OX1 3TH (GB).

(74) Agent: **J A KEMP LLP**; 80 Turnmill Street, London Greater London EC1M 5QU (GB).

(81) Designated States *(unless otherwise indicated, for every kind of national protection available)*: AE, AG, AL, AM, AO, AT, AU, AZ, BA, BB, BG, BH, BN, BR, BW, BY, BZ, CA, CH, CL, CN, CO, CR, CU, CV, CZ, DE, DJ, DK, DM, DO, DZ, EC, EE, EG, ES, FI, GB, GD, GE, GH, GM, GT, HN, HR, HU, ID, IL, IN, IQ, IR, IS, IT, JM, JO, JP, KE, KG, KH, KN, KP, KR, KW, KZ, LA, LC, LK, LR, LS, LU, LY, MA, MD, MG, MK, MN, MU, MW, MX, MY, MZ, NA, NG, NI, NO, NZ, OM, PA, PE, PG, PH, PL, PT, QA, RO, RS, RU, RW, SA, SC, SD, SE, SG, SK, SL, ST, SV, SY, TH, TJ, TM, TN, TR, TT, TZ, UA, UG, US, UZ, VC, VN, WS, ZA, ZM, ZW.

(84) Designated States *(unless otherwise indicated, for every kind of regional protection available)*: ARIPO (BW, CV, GH, GM, KE, LR, LS, MW, MZ, NA, RW, SC, SD, SL, ST, SZ, TZ, UG, ZM, ZW), Eurasian (AM, AZ, BY, KG, KZ, RU, TJ, TM), European (AL, AT, BE, BG, CH, CY, CZ,

(54) Title: SELECTIVE ENTRAINMENT OF NEURAL RHYTHMS BY NEURAL STIMULATION

Fig. 1

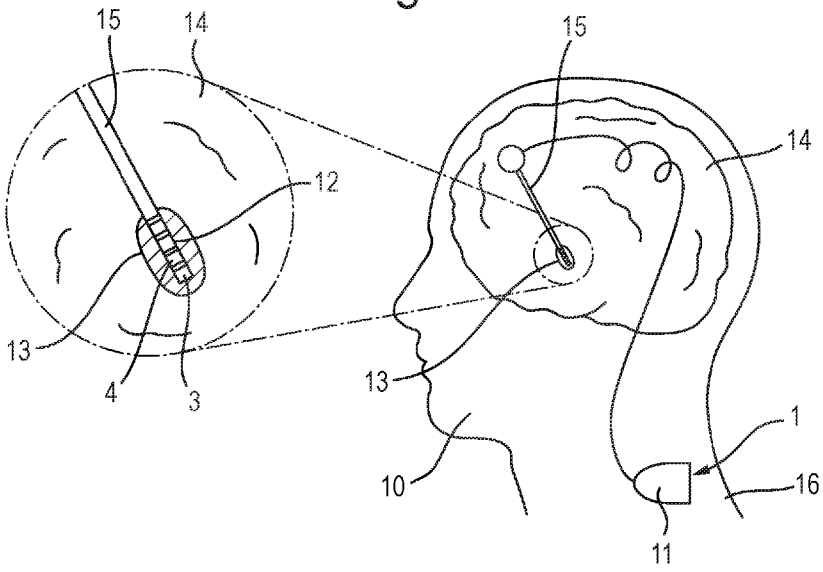


(57) Abstract: A stimulation device is used to entrain a target neural rhythm of a subject for treatment of the neurological disorder. A stimulation circuit generates a stimulation signal that is periodic and has stimulation periods that are dithered with an average period corresponding to an entrainment frequency of the target neural rhythm. As a result of the dither, neural stimulation using the stimulation signal causes entrainment of the target neural rhythm at the entrainment frequency and minimising entrainment of other neural rhythms at integer ratios of the entrainment frequency that may otherwise cause harmful effects.

WO 2024/003537 A1

*[Continued on next page]*

DE, DK, EE, ES, FI, FR, GB, GR, HR, HU, IE, IS, IT, LT, LU, LV, MC, ME, MK, MT, NL, NO, PL, PT, RO, RS, SE, SI, SK, SM, TR), OAPI (BF, BJ, CF, CG, CI, CM, GA, GN, GQ, GW, KM, ML, MR, NE, SN, TD, TG).

**Published:**

— *with international search report (Art. 21(3))*

Selective entrainment of neural rhythms by neural stimulation

The invention relates to entrainment of neural rhythms by neural stimulation.

In humans and animals, neural rhythms can be entrained non-invasively using periodic stimuli such as auditory stimulation, visual stimulation, or transcranial stimulation. Animal studies demonstrate that transcranial electrical stimulation can reliably entrain individual cortical neurons [13, 14], and can even entrain neurons in the hippocampus and the basal ganglia [15]. Additionally, rhythmic sensory stimulation in humans provides evidence for entrainment over the superposition of evoked responses [4, 2]. Deep brain stimulation (DBS), which invasively delivers electrical stimulation to deep targets in the brain, was also shown to entrain basal ganglia neurons in humans [16].

In line with this evidence and to develop new brain stimulation therapies for neurological disorders associated with neural rhythms, entraining neural rhythms has been suggested as a therapeutic mechanism to restore neurotypical behavior. Entraining individual alpha rhythms (8-12 Hz) using transcranial stimulation shows promise in patients with depression [17, 11] and chronic pain [18]. Gamma frequency (30-100 Hz) entrainment attenuates pathology associated with Alzheimer's disease and improves hippocampal function in mice [19, 20], and may favorably influence cognitive function as well as biomarkers of Alzheimer's-disease-associated degeneration in humans [21]. In patients with Parkinson's disease (PD), low-frequency switching of DBS between hemispheres entrains stepping, and could in principle be used to ameliorate gait impairment [23]. Transcranial alternating current stimulation at gamma frequency improves movement velocity in PD patients [23], likely by entraining the prokinetic gamma rhythm.

While brain stimulation therapies such as DBS for Parkinson's disease can be effective, they have yet to reach their full potential across neurological disorders. Similarly, entraining neural rhythms using rhythmic brain stimulation has been suggested as a new therapeutic mechanism to restore neurotypical behavior in conditions such as chronic pain, depression, and Alzheimer's disease.

However, theoretical and experimental evidence indicate that neural rhythms far from the stimulation frequency can also be inadvertently entrained by periodic brain stimulation, which, crucially, may lead to harmful effects. In patients with PD, finely-tuned gamma oscillations [24] can be entrained at half the frequency of DBS, which may be linked to debilitating involuntary movements known as dyskinesia [25-27]. In a study involving a canine with epilepsy, the frequency of DBS was chosen to avoid sub-harmonic

entrainment of rhythms associated with epileptic seizures [28]. Furthermore, sensory stimulation using visual flashes at 10 Hz can lead to super-harmonic entrainment [3], and was also reported to cause undesirable side effects as highlighted in a recent commentary [29]. Crucially, these counterintuitive effects can be harmful to patients, for example by triggering debilitating involuntary movements in Parkinson's disease, and thereby limit the efficacy of the therapy.

According to a first aspect of the invention there is provided a stimulation device for selective entrainment of a target neural rhythm of a subject, the stimulation device comprising a stimulation circuit arranged to generate a stimulation signal that is periodic and has stimulation periods that are dithered with an average period corresponding to an entrainment frequency of the target neural rhythm.

By dithering the stimulation periods in this manner, it has been shown that neural stimulation using the stimulation signal is capable of causing entrainment of the target neural rhythm at the entrainment frequency, while minimising entrainment of other neural rhythms at integer ratios of the entrainment frequency, in particular neural rhythms that have been identified as pathological. This provides for selective entrainment of the target neural rhythm.

As discussed in further detail below, the basis for this is as follows.

Due to the dithering, the stimulation signal remains periodic but the stimulation period varies instead of being constant (so the term "periodic" as used herein refers to the repeating nature of the stimulation signal, and does not imply a constant stimulation period). As the average period corresponds to an entrainment frequency of the target neural rhythm, the target neural rhythm is entrained, but the dithering minimises entrainment of other neural rhythms.

Synchronisation theory predicts that neural rhythms that are close to sub-harmonics and super-harmonics of the entrainment frequency of the target neural rhythm may be entrained by stimulation [30]. In neural networks, the possibility of sub- and super-harmonic entrainment has been corroborated by computational models [31-35, 27]. The frequency locking behaviour of a rhythm to external stimulation is characterised by its rotation number, which corresponds to the average number of cycles achieved by the rhythm between two periodic stimulation pulses. When the rotation number is rational, i.e of the form $\boldsymbol{p}$:$\boldsymbol{q}$ with $\boldsymbol{p}$ and $\boldsymbol{q}$ coprime integers, the rhythm is entrained by stimulation. Synchronisation regions in the stimulation frequency/amplitude space form characteristic patterns called Arnold tongues [36]. Arnold tongues at all possible integer ratios are

predicted for non-linear systems close to Hopf bifurcations [37]. However, among higher-order entrainment ratios ($\boldsymbol{p}$:$\boldsymbol{q}$ with $\boldsymbol{p} > \mathbf{1}$ and $\boldsymbol{q} > \mathbf{1}$), only the most stable ones (low $\boldsymbol{p}$ and $\boldsymbol{q}$) are likely to be observed in real neural systems. In keeping with this, experimental evidence of higher-order entrainment to brain stimulation is so far limited to the most stables higher-order ratios such as 1:2, 2:1, 3:1, and 4:1 [3, 38, 25, 26].

The target neural rhythm may be a neural rhythm for treatment of a neurological disorder. The present techniques may be applied to treat a broad range of neurological disorders. Such disorders include epilepsy, Parkinson's disease, multiple system atrophy, chronic pain, depression, dementia, and Alzheimer's disease, but these examples are not limitative and the applicability of techniques extends to any neurological disorder where there is an associated neural rhythm to entrain and pathological rhythms that should not be entrained. Such neural rhythms can occur across many timescales, and potentially impact circadian rhythms as well.

The target neural rhythm occurs in the nervous system of the subject. Often the target neural rhythm may occur in the brain of the subject, in which case it may be referred to as a brain rhythm. However, in general the target neural rhythm may occur in any part of the nervous system, as similar principles apply. As discussed below, when using the device, the neural rhythm may be monitored, but this is not essential.

In use of the device in neural stimulation, the neural stimulation signal is applied to the nervous system of the subject. Often, the neural stimulation signal may be applied to the brain of the subject, but in general the neural stimulation signal may be applied to any part of the nervous system, as similar principles apply. The neural stimulation signal may be applied to a part of the nervous system of the subject associated with the target neural rhythm, which may be the same or different physical location within the nervous system of the subject. The present techniques can be applied to any type of neural stimulation, the stimulation transducer being chosen accordingly. Some examples are as follows.

The present techniques have particular applicability to electromagnetic stimulation.

One example of electromagnetic stimulation is electrical stimulation, in which case the stimulation transducer may be an electrode. Examples of electrical stimulation include DBS, e.g. using electrodes implanted in the nervous system, and transcranial electrical stimulation, e.g. using electrodes that are located externally of the subject or implanted subdurally.

Another example of electromagnetic stimulation is magnetic stimulation, in which case the stimulation transducer may be a coil. Examples of magnetic stimulation include

transcranial magnetic stimulation, e.g. using external coils.

Other types of neural stimulation include acoustic stimulation, in which case the stimulation transducer may be an acoustic transducer, or optical stimulation, in which case the stimulation transducer may be an optical transducer.

Typically, the stimulation signal may comprises stimulation pulses.

In use of the stimulation device, the stimulation signal may be applied by a stimulation transducer. Thus, the stimulation device may further comprise a stimulation transducer arranged to receive the stimulation signal for applying the stimulation signal to the nervous system of the subject, or the stimulation device may be connected to such a stimulation transducer.

The nature of the dithering used to achieve the selective entrainment may be as follows.

The stimulation periods may be dithered by toggling between a predetermined set of stimulation periods. This simplifies the construction of the stimulation circuit as only a discrete number of stimulation periods need to be implemented.

To implement the random selection mentioned above, the stimulation periods may be randomly selected from the predetermined set of stimulation periods, which may average to a uniform distribution of each of the stimulation periods in the set in the case that the stimulation periods of the predetermined set are equally spaced and of equal probability. This is referred to herein as “random cycling” of the stimulation periods, although noting there is not a regular cycle.

The stimulation periods may be dithered with stimulation periods that have lengths varying in a predetermined cycle. This is referred to herein as “deterministic cycling” of the stimulation periods.

In one option, the predetermined cycle may comprise different lengths in each period of the stimulation signal. This is referred to herein as “fast deterministic cycling” of the stimulation periods.

In another option, the predetermined cycle comprises the same length in consecutive groups of periods. This is referred to herein as “slow deterministic cycling” of the stimulation periods.

In a different approach, the stimulation periods may be dithered with stimulation periods that are randomly selected from a predetermined distribution of stimulation periods. As an example of this, this may be implemented by adding white noise to a stimulation period corresponding to the entrainment frequency of the target neural rhythm,

which effectively corresponds to a normal distribution of stimulation periods.

In general, various forms of distributions of stimulation periods may be used.

The parameters of the distribution of stimulation periods may be selected to provide the selective entrainment.

In one type of example, the stimulation periods may be dithered with a distribution of stimulation periods that is symmetric, for example a uniform distribution (i.e. a rectangular distribution) or a non-uniform distribution, for example a normal distribution or a triangular distribution.

In another type of example, the stimulation periods may be dithered with a distribution of stimulation periods that is asymmetric. In this case, the distribution may have a value of Fisher's moment coefficient of skewness that is 0.2 or less.

The size of the distribution as represented by its standard deviation may similarly be selected to provide the selective entrainment.

In an example applicable to any form of distribution, the distribution may have a standard deviation of 0.5•Tavg or less, preferably $\sqrt{(1/12)}$ •Tavg or less, or more preferably 0.2•Tavg or less, where Tavg is the average length of the periods in the distribution.

In another example applicable to a uniform distribution, the distribution may have values in a range from 0.5.Tavg to 1.5Tavg, where Tavg is the average length of the periods in the distribution (which corresponds to standard deviation of $\sqrt{(1/12)}$ •Tavg or less).

The amplitude of the stimulation signal and/or one or more parameters of the dithering of the stimulation periods of the stimulation signal are selected to obtain entrainment of the target neural rhythm at a target level while maintaining entrainment of the other neural rhythms below a predetermined limit. This may be selected in advance of operating the stimulation device.

To allow calibration in use, the device may further comprise a control circuit arranged to receive a feedback signal representing measurements from the subject and to adjust the stimulation signal in response to the electrophysiological signal. Such a control circuit may be arranged to adjust the stimulation signal to obtain entrainment of the target neural rhythm at a target level while maintaining entrainment of the other neural rhythms below a predetermined limit.

In some cases, the feedback signal may be an electrophysiological signal representing neural rhythms of the subject. In this case, the electrophysiological signal may be any electrophysiological signal representing neural rhythms of the subject and in use

may be measured by a monitor transducer. Thus, the device may further comprise a monitor transducer arranged to measure the electrophysiological signal representing neural rhythms of the subject, or the stimulation device may be connected to such a monitor transducer.

For example, the electrophysiological signal may be a local field potential signal, in which case the monitor transducer may be electrodes implanted within the nervous system, or an electroencephalography (EEG) signal, in which case the monitor transducer may be electrodes that are located externally of the subject or implanted subdurally.

More generally, the feedback signal may represent other types of measurements of the subject, for example being measurements from a motion sensor or a pulse monitor.

The feedback signal may be a combinations of different types of measurement.

The adjustment of the stimulation signal may be adjustment of an amplitude of the stimulation signal and/or one or more parameters of the dithering of the stimulation periods of the stimulation signal.

The one or more parameters of the dithering of the stimulation periods of the stimulation signal may include the standard deviation of the distribution of the stimulation periods.

According to a second aspect of the present invention, there is provided a method of operating a neural stimulation device for selective entrainment of a target neural rhythm of a subject, the method comprising causing a stimulation circuit to generate a stimulation signal that is periodic and has stimulation periods that are dithered with an average period corresponding to an entrainment frequency of the target neural rhythm such that neural stimulation using the stimulation signal is capable of causing entrainment of the target neural rhythm at the entrainment frequency and minimising entrainment of other neural rhythms at integer ratios of the entrainment frequency.

Thus, the second aspect of the invention is a method corresponding to operation of the stimulation device in accordance with the first aspect of the present invention, and so provides the same advantages, as set out above. Similarly, the optional features of the first aspect of the invention set out above may also be applied to the second aspect of the present invention.

The method may further comprise: receiving a feedback signal representing measurements from the subject; and adjusting the stimulation signal in response to the feedback signal, for example to obtain entrainment of the target neural rhythm at a target level while maintaining entrainment of the other neural rhythms below a predetermined

limit. The adjustment of the stimulation signal may be adjustment of an amplitude of the stimulation signal and/or one or more parameters of the dithering of the stimulation periods of the stimulation signal, for example including the standard deviation of the distribution of the stimulation periods.

According to a third aspect of the present invention, there is provided a method of treatment of a neurological disorder of a subject, the method comprising: selecting a target neural rhythm for treatment of the neurological disorder; performing a method of operating a stimulation device according to the second aspect of the invention for entrainment of the target neural rhythm; and applying the stimulation signal to the nervous system of the subject.

Thus, the third aspect of the invention is a method of treatment that incorporates operation of the stimulation device in accordance the first aspect of the present invention, and so provides the same advantages, as set out above. Similarly, the optional features of the first aspect of the invention set out above may also be applied to the third aspect of the present invention.

Embodiments of the invention will now be described, by way of non-limitative example, with reference to the accompanying drawings in which:

Fig. 1 is a diagram of a stimulation device for DBS;

Fig. 2 is a block diagram of the electronic components of the stimulation device of Fig. 1;

Fig. 3 is a circuit diagram of the frequency synthesiser of a stimulation circuit of Fig. 2;

Fig. 4 is a flow chart of a method of treatment of a neurological disorder of a subject using the stimulation device of Fig. 1;

Fig. 5 is a flow chart of a method of adjusting the stimulation signal generated by the stimulation device of Fig. 1;

Fig. 6 is a set of plots and graphs illustrating selective entrainment of neural rhythms using DBS, Figs. 6D1 and 6D2 being waveforms of stimulation signals with and without dithering, Figs. 6C1 and 6C2 being plots of stimulation amplitude against natural frequency for the two waveforms showing Arnold tongues according to the sine circle map model, Figs. 6B1-6B4 being plots of neural rhythms frequency-locked to stimulation at various ratios in Figs. 6C1 and 6C2, and Fig. 6A being a plots of cortical gamma power spectral density against frequency with and without DBS in PD patients (adapted from [25]);

Fig. 7 is a set of graphs of rotation number against natural frequency for several frequency locking plateaux and various dithering levels in the sine circle map model;

Fig. 8 is a set of plots and graphs for different levels of dithering and associated graphs, Figs. 8A being plots of stimulation amplitude against natural frequency showing Arnold tongues for waveforms with increasing dithering levels, Fig. 8B being graphs of normalised tongue width against dithering level for three stimulation amplitudes, Fig. 8C being graphs of tongue width obtained by simulation and theory against dithering level for three stimulation amplitudes, and Fig. 8D being graphs of tongue width obtained by simulation and theory against stimulation amplitudes for three dithering levels;

Fig. 9 is a set of plots of Arnold tongues for different levels of dithering and associated graphs, Figs. 9A1-9A4 being plots of stimulation amplitude against natural frequency showing Arnold tongues; Figs. 9B1-9B4 being plots of tongue width as a function of stimulation amplitude, and Figs. 9C1-9C4 being plots of mean instantaneous frequency in the natural frequency/stimulation amplitude space;

Fig. 10 is a set of waveforms of three dithered stimulation signals generated by toggling between a predetermined set of stimulation periods, Fig. 10A showing random cycling, Fig. 10B showing fast deterministic cycling and Fig. 10C showing slow deterministic cycling;

Fig. 11 is a set of plots and graphs showing Arnold tongues for different types of toggling between a predetermined set of stimulation periods, Figs. 11A1-11A6 showing frequency locking regions in the natural frequency/stimulation amplitude space, Figs. 11B1-11B6 being graphs of tongue width against stimulation amplitude and Figs. 11C1-11C6 being plots of mean instantaneous frequency in the natural frequency/stimulation amplitude space;

Fig. 12 is four Cobweb plots of the deterministic sine circle map for different frequency locking ratios;

Fig. 13 is a set of graphs of stimulation amplitude against natural frequency showing Arnold tongues with values of the integer ratio of up to 4 for increasing dithering levels;

Fig. 14 is a graph of tongue widths obtained by simulation and theory against dithering level showing Arnold tongues with integer ratios up to 4;

Fig. 15 is a set of plots of Arnold tongues for different levels of dithering and associated graphs, Figs. 15A1-15A6 being plots of frequency locking regions in the natural frequency/stimulation amplitude space, Figs. 15B1-15B6 being plots of phase-locking

value (PLV) for p:1 locking in the natural frequency/stimulation amplitude space, Figs. 15C1-15C6 being plots of PLV for p:2 locking in the natural frequency/stimulation amplitude space and Figs 15D1-15D6 being plots of PLV for $(2p-1)$:2 locking in the natural frequency/stimulation amplitude space;

Fig. 16 is a set of plots of Arnold tongues for different levels of dithering and associated graphs, Figs. 16A1-16A6 being plots of frequency locking regions in the natural frequency/stimulation amplitude space, Figs. 16B1-16B6 being plots of PLV for p:1 locking in the natural frequency/stimulation amplitude space, Figs. 16C1-16C6 being plots of PLV for p:2 locking in the natural frequency/stimulation amplitude space and Figs 16D1-16D6 being plots of PLV for $(2p-1)$:2 locking in the natural frequency/stimulation amplitude space; and

Fig. 17 shows Kuramoto model outputs in the absence of stimulation for two different frequencies, Figs 17A1 and 17A2 being plots of the output over time, Fig. 17B being a graph of the PRC of the oscillators and Fig. 17C being a plot of charge-balanced rectangular stimulation pulse used in simulations.

Fig. 1 shows a stimulation device 1 for selective entrainment of a target neural rhythm using DBS of a subject 10 as an example of neural stimulation. The subject is shown as a human in Fig. 1, although in general could be a human or an animal. The stimulation device 1 is arranged as follows.

The stimulation device 1 comprises a unit 11 housing a stimulation circuit 20 that generate a stimulation signal, as described further below with reference to Fig. 2.

The stimulation device 1 also comprises an electrode arrangement 12 comprising stimulation electrodes 3 and monitor electrodes 4. The electrode arrangement 12 is formed on the tip of a guide wire 15 that makes parallel electrical connection between the stimulation circuit 20 in the unit 11 and the individual stimulation electrodes 3 and monitor electrodes 4. In general, any suitable number of stimulation electrodes 3 and monitor electrodes 4 may be provided, the number shown in Fig. 1 being a non-limitative example.

For use in DBS, the stimulation device 1 is implanted as follows.

The electrode arrangement 12 is surgically implanted into a target region 13 in the brain 14 of the subject 10 through a small opening in the skull of the subject 10. The unit 11 is shown as being implanted into the thorax 16 of the subject 10 near the collarbone, with the lead wire 15 extending under the skin of the patient 10, but other implantation locations are possible for example directly in the skull of the subject 10.

Although in this example the electrode arrangement 12 is implanted in the brain 14

for DBS, in general the electrode arrangement 12 could be implanted in any part of the nervous system of the subject 10.

The stimulation circuit 20 supplies the stimulation signal to the stimulation electrodes 3 and apply the stimulation signal as electrical stimulation to the target region 13. Thus, in this example, the stimulation electrodes 3 are stimulation transducers.

The monitor electrodes 4, which form monitor transducers in this example, measure a local field potential (LFP) signal from the target region 13 which is received by the stimulation circuit 20. The LFP signal represents neural rhythms of the subject 10. Thus, in this example, the LFP signal is the electrophysiological signal and the monitor electrodes 4 are monitor transducers. Both healthy neural rhythms and pathological neural rhythms may be identified using the LFP signal.

Various configurations for the monitor electrodes 4 are possible. In some examples, the monitor electrodes 4 may be bundled with the stimulation electrodes 4 in a common transducer pad. In some examples, electrodes of the electrode arrangement 12 may be operable as both stimulation electrodes 3 and monitor electrodes 4.

The stimulation device 1 is provided with a ground that is normally placed far away from the electrode arrangement 12. When the overall deep brain stimulation (DBS) is internalised, the ground 10 may be connected to the housing of the unit 11 implanted under the skin at the thoracic level, although during externalisation, e.g. for research purpose, the ground 10 may be taken from a part of the skin that minimises electrocardiogram (ECG) artefacts, such as the arm, neck or shoulder.

Fig. 2 shows the stimulation circuit 20 of the stimulation device 1, which is arranged as follows.

The stimulation circuit 20 comprises a frequency synthesiser 21 and a pulse generator 22.

The frequency synthesiser 21 generates a clock signal that is supplied to the pulse generator 22.

The pulse generator 22 generates the stimulation signal as pulses at timings controlled by the clock signal. Thus, the stimulation signal is periodic and has a stimulation period that is equal to the period of the clock signal. The stimulation frequency is the inverse of the stimulation period, and so references herein to the stimulation period (or frequency) may be replaced by references to the corresponding stimulation frequency (or period).

The pulses may in general have any suitable waveform. Typically, the pulses

comprise a bipolar pulse sequence in each stimulation period for the purpose of charge balancing of the target region. The pulses may have a rectangular waveform for ease of generation by switching of a voltage source.

The stimulation signal is supplied from the pulse generator 22 to the stimulation electrodes 3.

The stimulation circuit 20 also comprises a control unit 23 that controls the frequency synthesiser 21 and the pulse generator 22. The control unit 23 controls the frequency synthesiser 21 to select the period of the clock signal and thereby to adjust the stimulation period. The control unit 23 controls the pulse generator 22 to adjust parameters of the individual pulses, such as their amplitude and optionally their waveform. The control unit 23 also receives the LFP signal from the monitor electrodes 4.

The stimulation circuit 20 also comprises a sensor 5 which takes measurements from the subject 10. The sensor 5 may be of any type, for example being a motion sensor that measures motion of the subject 10, e.g. an accelerometer, or a pulse sensor that measures the pulse of the subject 10. More generally, plural sensors 5 of different types may be provided. The control unit 23 also receives the measurements from the sensor 5 (or plural sensors 5, if provided) as a feedback signal.

Fig. 3 shows the frequency synthesiser 21, which has a conventional arrangement as follows.

The frequency synthesiser 21 comprises a master oscillator 30, a phase-locked loop 31 and a frequency controller 32. The master oscillator 30 generates a master clock signal and supplied it to the phase-locked loop 31.

The phase-locked loop 31 comprises a voltage controlled oscillator 33, a frequency divider 34, a phase comparator 35 and a low pass filter 36. The voltage controlled oscillator 33 generates the clock signal that is output by the frequency synthesiser 21. The clock signal is also supplied to the frequency divider 34, which frequency divides the clock signal to provide a frequency-divided signal that is supplied to the phase comparator 35. The phase comparator 35 compares the phases of the master clock signal and the frequency-divided signal and outputs an error signal that represents the phase error therebetween. The error signal is supplied through the low pass filter to the voltage controlled oscillator 33, which controls the frequency of the clock signal so as to reduce the error signal.

In this manner, the clock signal has a period that is controlled by the frequency division ratio of the frequency divider 34. This frequency division ratio is set by the

frequency controller 32 to set the stimulation period. The frequency controller 32 receives the clock signal from the phase-locked loop and synchronises changes in the frequency division ratio with the clock signal. The control unit 23 controls the frequency controller 32 to set the frequency division ratio, and hence the stimulation period.

Optionally, a further frequency divider may be provided between the phase-locked loop 31 and the frequency controller 32, and may have a frequency division ratio set by the frequency controller 32, under the control of the control unit 32, to provide a further degree of control of the stimulation period.

Fig. 4 shows method of treatment of a neurological disorder of a subject, which is performed as follows.

In step S1, a target neural rhythm for treatment of the neurological disorder is selected. The target neural rhythm is a neural rhythm that is associated with the neurological disorder. As discussed above, the present techniques may be applied to any neurological disorder having an associated neural rhythm that can be entrained for treatment of the disorder, non-limitative examples including epilepsy, Parkinson's disease, multiple system atrophy, chronic pain, depression, dementia, and Alzheimer's disease. The frequency of the target neural rhythm is the entrainment frequency.

In step S2, the stimulation device 1 is operated to generate a stimulation signal for entrainment of the target neural rhythm. The stimulation periods of the stimulation signal is controlled by the control unit 23, in the manner discussed above. As discussed in more detail below, the stimulation signal has stimulation periods that have an average period corresponding to an entrainment frequency of the target neural rhythm, but are dithered around that average period in order to avoid entraining other neural rhythms than the target rhythm. As a result of the dithering, the stimulation signal remains periodic but the stimulation period varies instead of being constant (so the term "periodic" as used herein refers to the repeating nature of the stimulation signal, and does not imply a constant stimulation period). As the period of the stimulation signal is dithered, herein the stimulation signal is referred to as a "dithered stimulation signal". Such dither of the period of the stimulation signal may alternatively be referred to as jitter of the stimulation signal. As such, references herein to the period of the stimulation signal being dithered may be replaced by references to jitter being applied to the period of the stimulation signal, and similarly references to a "dithered stimulation signal" may be replaced by references to a "jittered stimulation signal".

In step S3, the stimulation signal generated by the stimulation device 1 is supplied

to the stimulation electrodes 3 which apply the stimulation signal as electrical stimulation to the target region 13 of the brain 14, and thereby entrain the target neural rhythm to provide treatment of the neurological disorder.

The dithering of the stimulation periods of the stimulation signal causes selective entrainment of the target neural rhythm. Such entrainment also occurs at a range of frequencies around the frequency of the target neural rhythm (as shown by the width of the Arnold tongues in Fig. 6 and other drawings discussed below). This entrainment of the target neural occurs, while minimising entrainment of other neural rhythms that would otherwise occur at integer ratios of the entrainment frequency, in particular other neural rhythms that have been identified as pathological. As mentioned above for the target neural rhythm, such entrainment would also otherwise occur at a range of frequencies around the frequency of the target neural rhythm (as shown by the width of the Arnold tongues in Fig. 6 and other drawings discussed below). The basis for this effect will now be explained.

Reference is made to Fig. 6, which is a set of plots and graphs illustrating selective entrainment of neural rhythms.

When stimulation is perfectly periodic as depicted in Fig. 6D1 (wherein $f_s$ denotes the stimulation frequency), neural oscillators may be entrained at the stimulation frequency but also at sub- and supra-harmonics of the stimulation frequency. Corresponding entrainment regions (Arnold tongues) are represented in Fig. 6C1 for uncoupled neural oscillators modelled using the sine circle map. Stimulation is provided at 130 Hz (vertical dashed line), with stimulation amplitude shown on the vertical axis, and the natural frequency of oscillators on the horizontal axis. Entrainment is observed when the rotation number (graded scale in Fig. 6C) is an integer ratio (only regions of frequency-locking determined as described in the Methods Section below). Entrainment at various rotation numbers is illustrated in Figs. 6B1-6B4.

As an example, DBS in PD patients can entrain cortical gamma oscillations at half the stimulation frequency, which corresponds to 1:2 entrainment (as shown in Fig. 6A, adapted from [25]). With dithering, stimulation is not perfectly periodic (Fig. 6D2), and past a certain level of noise in the stimulation period, only the 1:1 Arnold tongue subsists (green tongue in Fig. 6C2).

The present approach to selective entrainment using dithered stimulation rests on the fact that entrainment is the most stable around the stimulation frequency. In other words, 1:1 entrainment is generally more stable than $p{:}q$ entrainment for $p > 1$ and $q > 1$. Small changes in oscillator frequency do not affect the 1:1 Arnold tongue much, while

higher-order Arnold tongues are less stable to perturbations. This is also true for small changes in stimulation frequency. Therefore, introducing variations in the stimulation frequency perturbs frequency locking more for higher-order tongues than for 1:1 entrainment. This is the basis of the dithering approach to selective entrainment, which consists in its simplest form in adding white noise to the stimulation period, as illustrated in Fig. 6D2. Here, an open loop stimulation pattern is considered where the time interval between stimulation pulses always changes and is given by $(1 + z)/f_s$, where $f_s$ is the base stimulation frequency, and $z$ is a normal random number sampled from $\mathcal{N}(0, \zeta^2)$ for each stimulation interval. The standard deviation $\zeta$ is termed herein the "dithering level". Past a certain dithering level, only the 1:1 Arnold tongue remains (Fig. 6C2), which ensures that only neural rhythms of frequency close to the stimulation frequency are entrained. By adjusting $f_s$ to the target rhythm to entrain, selective entrainment can therefore be achieved using dithered stimulation.

Theoretical and computational demonstrations of the efficacy of the method are provided next.

First it is shown that selective entrainment can be achieved by dithered stimulation in models of uncoupled neural oscillators

The sine circle map is the simplest model describing the influence of periodic stimulation on a single neural oscillator, and can be used to provide a theoretical basis for the efficacy of dithered stimulation as a selective entrainment strategy. The model maps the phase of an oscillator right before stimulation pulse $n$ (denoted $\theta_n$) to the phase of the oscillator right before stimulation pulse $n + 1$ (denoted $\theta_{n+1}$). The map can be written as:

$$\boldsymbol{\theta_{n+1} = \theta_n + 2\pi\frac{f_0}{f_s} + I\sin\theta_n = F(\theta_n)} \quad \mathbf{(1)}$$

where $f_0$ is the oscillator natural frequency, $f_s$ the stimulation frequency, and $I$ the stimulation magnitude. Entrainment can arise because a stimulus may advance or delay the phase of an oscillator depending on the phase at which it is applied. This concept is captured by the phase response curve (PRC) of the oscillator, which describes the change in phase of the oscillator as a function of the stimulation phase. The PRC of the sine circle map is a simple sinusoid ($Z(\theta) = \sin\theta$). Since brain oscillations can manifest across a wide range of frequencies, a population of uncoupled neural oscillators can be modelled by equation (1) where $f_0$ corresponds to the natural frequency axis in Fig. 6C1. For perfectly periodic stimulation, Arnold tongues are observed in Fig. 6C1 at all possible entrainment ratios (rotation number obtained as detailed below).

When representing the rotation number as a function of natural frequency, frequency locking corresponds to plateaux where the rotation number takes a constant integer ratio across a range of natural frequencies as illustrated in Fig. 7 (discussed below) for $\zeta = 0$ (only ratios with low $p$ and $q$ are easily discernable).

A theoretical justification of dithering stimulation as a selective entrainment strategy is as follows.

To demonstrate analytically that dithered stimulation destabilises the most prominent higher-order entrainment ratios more than 1:1 entrainment, dithered stimulation is introduced in the sine circle map. The sine circle map with dithered stimulation becomes the stochastic map:

$$\boldsymbol{\theta_{n+1} = \theta_n + 2\pi\frac{f_0}{f_s}(1 + z_n) + I\sin\theta_n = F(\theta_n) + 2\pi\frac{f_0}{f_s}z_n} \quad (2)$$

where the stimulation period $T_s = 1/f_s$ is multiplied by $(1 + z_n)$ to model dithered stimulation, with $z_n$ normal random numbers sampled from $\mathcal{N}(0, \zeta^2)$.

The ideas presented in [43] are built on to show that, as more dithering is introduced in equation (2), the relative decrease in width of the most prominent higher-order Arnold tongues is greater than that of the 1:1 tongue. The most prominent higher-order tongues are of the form $\boldsymbol{p}$:1 with $\boldsymbol{p > 1}$ (supra-harmonic entrainment), and $(\boldsymbol{2p - 1})$:2 with $\boldsymbol{p \geq 1}$. In Fig. 6C1, these correspond to the 2:1 tongue, and to the 1:2 and 3:2 tongues, respectively. Herein, $\boldsymbol{\Delta f^{p:q}(I, \zeta)}$ denotes the range of oscillator natural frequencies that can be entrained by the $\boldsymbol{p}$:$\boldsymbol{q}$ tongue with dithered stimulation of amplitude $\boldsymbol{I}$ and dithering level $\boldsymbol{\zeta}$, i.e. the width of the tongue at that stimulation amplitude and dithering level. Approximate expressions for $\boldsymbol{\Delta f^{p:1}(I, \zeta)}$, $\boldsymbol{p \geq 1}$ and $\boldsymbol{\Delta f^{(2p-1):2}(I, \zeta)}$, $\boldsymbol{p \geq 1}$ are derived in the Methods Section below assuming $\boldsymbol{\zeta \ll 1}$ and $\boldsymbol{I \ll 1}$. Neglecting small high order $\boldsymbol{I}$ terms in equation (7) in the Methods Section below, the width of $\boldsymbol{p}$:1 tongues ($\boldsymbol{p \geq 1}$) with dithered stimulation relative to the width of the same tongues with perfectly periodic stimulation can be obtained as:

$$\boldsymbol{\frac{\Delta f^{p:1}(I, \zeta)}{\Delta f^{p:1}(I, 0)} \approx 1 - \frac{n_\sigma^2 \pi^2 p^2}{2}\zeta^2} \quad (3)$$

where $n_\sigma$ quantifies the number of standard deviations of the jump distribution beyond which temporary escapes of the basin of attraction of the periodic orbit are considered to not significantly affect the locking behavior (see the Methods Section below for more details). The value of $n_\sigma$ is taken to be the same across tongues. Similarly, neglecting high order $I$ terms in equation (10) in the Methods Section below, the width of $(2p - 1)$:2

tongues ($p \geq 1$) with dithered stimulation relative to the width of the same tongues with perfectly periodic stimulation is:

$$\frac{\Delta f^{(2p-1):2}(I,\zeta)}{\Delta f^{(2p-1):2}(I,0)} \approx 1 - n_\sigma^2 \pi^2 (2p-1)^2 \zeta^2 \qquad (4)$$

It follows that the relative decrease of the most prominent higher-order tongues (any $p > 1$ in equation (3) and any $p \geq 1$ in equation (4)) with increasing dithering levels is always greater than for the 1:1 tongue ($p = 1$ in equation (3)). This result is valid for any stimulation frequency and underlies the efficacy of dithered stimulation for selective entrainment.

Validation using simulations of uncoupled neural oscillators is now presented.

To confirm that there exists a dithering level at which the 1:1 tongue displays a broad frequency locking region while other tongues have disappeared, the sine circle map is simulated with dithered stimulation (equation (2)) for increasing noise levels. As an example, the base stimulation frequency is set to $f_s = 130$ Hz, which corresponds to the frequency of clinically available DBS.

Fig. 8 shows that Arnold tongues disappear faster for higher order entrainment than for 1:1 entrainment with increasing dithering level in uncoupled neural oscillators. Fig. 8A shows frequency locking regions in the oscillator frequency/stimulation amplitude space. Only regions of frequency-locking (determined as presented in the Methods Section below), known as Arnold tongues, are shown. The graded scale represents the rotation number. Dithering level increases from top to bottom, and theoretical tongue boundaries (equations (6) and (9) are shown by black dashed lines. The stimulation frequency is indicated by a red dashed line. Fig. 8B shows theoretical tongue width normalised by its value for perfectly periodic stimulation, plotted against dithering level, for three stimulation amplitudes. The dependence on stimulation amplitude is very slight. Fig. 8C compares tongue width obtained from theory and simulations, as a function of dithering level, for three stimulation amplitudes. Fig. 8D compares tongue width obtained from theory and simulations, as a function of stimulation amplitude, for three dithering levels. In all panels showing data from simulations, for each natural frequency, stimulation amplitude, and dithering value, the rotation number is averaged over 10 repeats, with $10^4$ stimulation pulses per repeat. In Figs. 8B-8D, theoretical tongue widths refer to equations (7) and (10).

As ζ is increased, frequency locking plateaux in Fig. 7 disappear faster for higher order entrainment than for 1:1 entrainment. Significant 1:1 frequency locking is still

possible for $\zeta = 0.009$ as indicated by the large dashed line plateau in Fig. 7C, but no 1:2, 3:2, or 2:1 frequency locking is possible (Fig. 7B, 7D, 7E). Similarly, higher order Arnold tongues become narrower faster than the 1:1 tongue as $\zeta$ is increased (Fig. 8A1-8A4). For $\zeta = 0.009$, the 1:1 tongue can still entrain neural oscillators with natural frequencies in the vicinity of the stimulation frequency, while other tongues have disappeared (Fig. 8A4). This is consistent with the faster relative decrease in width of higher order tongues compared to the 1:1 tongue (Fig. 8B).

Simulations of the sine circle map with dithered stimulation also validate the theoretical results. Specifically, equations (6) and (9) in the Methods Section below describing tongue boundaries in the presence of dithered stimulation (dashed lines in Figs. 8A1-8A4) approximately match tongue boundaries obtained directly from simulations. Additionally, tongue width measurements from simulations approximately match theoretical values from equations (7) and (10) in the Methods Section below as shown in Fig. 8C-8D.

Fig. 7 shows that frequency locking plateaux disappear faster for higher-order entrainment than for 1:1 entrainment with increased dithering. In Fig. 7, solid lines correspond to perfectly periodic stimulation, while dashed/dotted lines correspond to dithered stimulation with increasing dithering levels.

While a large part of the 1:1 frequency locking plateau is preserved for all dithering levels shown (Fig. 7C), plateaux for 1:2 (Fig. 7B), 3:2 (Fig. 7D), and 2:1 (Fig. 7E) frequency locking have disappeared at $\zeta = 0.09$. Fig. 7B-7E are zoomed-in versions of Fig. 7A. For each dithering level, the rotation number is averaged over 10 repeats, with $10^4$ stimulation pulses per repeat.

It has also been confirmed that the theoretical results hold for $\boldsymbol{p}$:1 tongues and $(\boldsymbol{2p-1})$:2 tongues for larger values of $\mathbf{p}$ as shown in Figs. 13 and 14.

Fig. 13 shows $\mathbf{p}$:1 and $(\mathbf{2p-1})$:2 Arnold tongues with $\mathbf{p}$ up to 4, and validate theoretical results and the efficacy of dithered stimulation. Fig. 13 represents frequency locking regions in the oscillator frequency/stimulation amplitude space. Only regions of frequency-locking (determined as presented in the Methods Section below), are shown in color. The color scale represents the rotation number. Dithering level increases from top to bottom, and theoretical tongue boundaries (equations (6) and (9)) are shown by black dashed lines. The stimulation frequency is indicated by a red dashed line. For each natural frequency, stimulation amplitude, and dithering value, the rotation number is averaged over 10 repeats, with $\mathbf{10^4}$ stimulation pulses per repeat. Higher dithering levels, resulting

in only the 1:1 tongue being stable, are shown in Fig. 8A.

Fig. 14 shows the width of $\mathbf{p}$:1 and $(\mathbf{2p-1})$:2 Arnold tongues with $\mathbf{p}$ up to 4, and compares simulations and theoretical results. Comparing tongue width obtained from equations (7) and (10) and simulations, as a function of the dithering level, for $\mathbf{I=1}$. For each natural frequency and dithering value, the rotation number from simulations is averaged over 10 repeats, with $\mathbf{10^4}$ stimulation pulses per repeat. Higher dithering levels, resulting in only the 1:1 tongue being stable, are shown in Fig. 8C2.

As predicted, these tongues disappear for even lower dithering levels than the tongues in Fig. 8. In Figs. 8, 13 and 14, theoretical results were based on $\boldsymbol{n_\sigma = 4}$, i.e. frequency-locking was considered to occurs when at least 99.99% of locking cycles do not escape the periodic orbit. This was found to robustly correspond to frequency-locking plateaux in Fig. 7 across noise levels.

Although a range of dithering levels that suppress the 1:2 tongue while still preserving the 1:1 tongue were found (Fig. 8A4), it is noted that the 1:2 tongue is the hardest higher-order tongue to destabilise (see Fig. 8B2 and 8C2). The fact that 1:2 entrainment was the first type of higher-order entrainment reported in patients with Parkinson's disease treated with DBS [25, 26] is in line with these predictions.

It is shown that the efficacy of dithered stimulation as a selective entrainment strategy is supported by theory, and confirmed by simulations of uncoupled neural oscillators. However brain signals such as local field potentials can be better described by networks of coupled oscillators representing coupled neurons or coupled micro-circuits [44-46]. Thus, dithered stimulation was tested in this more realistic setting.

It is now shown that selective entrainment can be achieved by dithering in populations of coupled neural oscillators.

In order to test dithered stimulation as a selective entrainment strategy in a more realistic setting, populations of coupled neural oscillators are simulated using the Kuramoto model [47]. For each natural frequency $f_0$ in the frequency range of interest, thre is considered a population of $M = 100$ phase oscillators with homogeneous coupling, natural frequencies distributed around $f_0$, and the PRC of a standard Hodgkin-Huxley neuron [48, 49] (see Fig. 17B1). Full details on the model can be found in the Methods Section below. As opposed to the sine circle map, the Kuramoto model is a continuous-time model. Thus, it is possible to use more realistic, square stimulation pulses with a temporal extent, and a negative component for charge balance (see the Methods Section below and Fig. 17B2).

Fig. 9 shows that Arnold tongues disappear faster for higher-order entrainment than for 1:1 entrainment with increasing dithering in populations of coupled neural oscillators. Dithering level increases from the top row to the bottom row. Fig. 9A shows frequency locking regions in the natural frequency/stimulation amplitude space. Only regions of frequency-locking (determined as presented in the Methods Section below) are shown. The graded scale represents the rotation number. Fig. 9B shows Arnold tongue width as a function of stimulation amplitude. Fig. 9C shows mean instantaneous frequency (represented by the graded scale) in the natural frequency/stimulation amplitude space. In Figs. 9A and 9C, for each natural frequency, stimulation amplitude, and dithering value, the rotation number or mean instantaneous frequency are averaged over 5 repeats, with 400 stimulation pulses per repeat. The stimulation frequency is indicated by a dashed line.

As shown in Fig. 9, dithered stimulation is an effective selective entrainment strategy in populations of coupled neural oscillators. For perfectly periodic stimulation at 130 Hz, populations of coupled neural oscillators can be entrained at the stimulation frequency (1:1 entrainment), but also at higher-order entrainment ratios for certain natural frequencies and stimulation amplitudes (Fig. 9A1). In the natural frequency range considered, the only higher-order tongues with non-zero widths are the 1:2, 3:2, and 2:1 tongues, which were identified as the most prominent higher-order tongues in the sine circle map. As the dithering level $\boldsymbol{\zeta}$ is increased, these higher-order tongues fade, while the 1:1 tongue is mostly preserved (Fig. 9A1-A4). For $\boldsymbol{\zeta = 0.15}$, 1:1 entrainment is maintained for a large range of natural frequencies and stimulation amplitudes, while higher order entrainment has vanished (Fig. 9A4). This is confirmed by measuring the width of Arnold tongues as a function of stimulation amplitude (Fig. 9B4). The variation in the mean instantaneous frequency of the Kuramoto populations with respect to $\boldsymbol{f_0}$ also supports this conclusion. For $\boldsymbol{\zeta = 0.15}$, the mean instantaneous frequency is constant in the 1:1 tongue, signalling frequency-locking to the stimulation frequency, while a non-zero frequency gradient along $\boldsymbol{f_0}$ is observed elsewhere, indicated the absence of frequency-locking (Fig. 9C4). This was not the case for the perfectly periodic case, where regions of constant mean instantaneous frequency can be seen to approximately match the 1:2, 3:2, and 2:1 tongues (Fig. 9C1). Details on how entrainment metrics presented in Fig. 9 are obtained can be found in the Methods Section below. Further validation is provided in Fig. 15 based on the phase locking value (PLV), which was used to assess 1:1 synchronisation for example in [6, 50].

These results are confirmed by PLV analysis illustrated in Fig. 15, which shows the

efficacy of dithered stimulation by PLV analysis in populations of coupled neural oscillators. Dithering level increases from the top row to the bottom row. 15A1-15A6 show Frequency locking regions in the natural frequency/stimulation amplitude space. Only regions of frequency-locking (determined as presented in the Methods Section below) are shown. The graded scale represents the rotation number. Figs. 15B1-15B6 show PLV $\boldsymbol{p}$:1 (graded scale) in the natural frequency/stimulation amplitude space. Here, PLV $\boldsymbol{p}$:1 detects 1:1 and 2:1 entrainment. Figs. 15C1-15C6 show PLV $\boldsymbol{p}$:2 (graded scale) in the natural frequency/stimulation amplitude space. Here, PLV $\boldsymbol{p}$:2 detects 1:2 and 3:2 entrainment, but also 1:1 and 2:1 entrainment. Figs. 15D1-15D6 show PLV $(\boldsymbol{2p-1})$:2 (color scale) in the natural frequency/stimulation amplitude space, obtained as PLV $\boldsymbol{p}$:2 - PLV $\boldsymbol{p}$:1. Here, PLV $(\boldsymbol{2p-1})$:2 detects 1:2 and 3:2 entrainment.

In all panels, for each natural frequency, stimulation amplitude, and dithering value, the rotation number or mean instantaneous frequency is averaged over 5 repeats, with $\boldsymbol{400}$ stimulation pulses per repeat. The stimulation frequency is indicated by red dashed lines. For $\boldsymbol{\zeta = 0.15}$, 2:1 entrainment has disappeared while 1:1 entrainment is still supported (compare Fig. 15B4 to Fig. 15B1). 1:2 and 3:2 entrainment have also disappeared (compare Fig. 1D4 to Fig. 15D1).

The PLV is calculated in the Kuramoto model as:

$$\text{PLV } \boldsymbol{p}\text{:1} = \frac{\boldsymbol{1}}{\boldsymbol{N}}\left|\sum_{\boldsymbol{k=1}}^{\boldsymbol{N}} \boldsymbol{e^{i\psi(t_k)}}\right|$$

and quantifies the phase concentration of the order parameter at the time of stimulation, considering all stimulation pulses. PLV $p$:1 will therefore detect $p$:1 entrainment, for any $p \geq 1$. There is also considered:

$$\text{PLV } \boldsymbol{p}\text{:2} = \frac{\boldsymbol{1}}{\left\lfloor \frac{\boldsymbol{N}}{\boldsymbol{2}} \right\rfloor}\left|\sum_{\boldsymbol{k=1}}^{\boldsymbol{\lfloor N/2 \rfloor}} \boldsymbol{e^{i\psi(t_{2k})}}\right|,$$

with $\lfloor . \rfloor$ the floor function. PLV $p$:2 only considers every other stimulation pulse, and will detect $p$:2 entrainment ($p \geq 1$), which includes for example 1:2 and 3:2 entrainment, but also 1:1 and 2:1 entrainment. Thus, to only detect $(2p-1)$:2 entrainment (in particular the 1:2 and 3:2 tongues), then PLV $(2p-1)$:2 = PLV $p$:2 − PLV $p$:1.

Fig. 17 shows Kuramoto model outputs in the absence of stimulation; PRC and stimulation pulse. Example outputs from the Kuramoto model for the chosen parameters in the absence of stimulation for $\boldsymbol{f_0 = 30}$ Hz (A1) and $\boldsymbol{f_0 = 185}$ Hz (A2). The PRC of the

oscillators is taken from the standard Hodgkin-Huxley neuron model (B1). The charge-balanced rectangular stimulation pulse used in simulations is shown in B2 ($T_s$ is the stimulation period). The pulse shown has an energy of 1 a.u. over $T_s$, and is taken to be the base pulse for a stimulation amplitude of 1 a.u. in simulations.

The dithering may be applied in various different ways to achieve the selective entrainment. Some examples are as follows.

In a simple approach, the stimulation periods may be dithered with stimulation periods that are randomly selected from a predetermined distribution of stimulation periods.

As an example of this, this may be implemented by adding white noise to the stimulation period corresponding to the entrainment frequency of the target neural rhythm, which effectively corresponds to a normal distribution of stimulation periods (i.e. a rectangular distribution).

Alternatively, the stimulation periods may be dithered by toggling between a predetermined set of stimulation periods, i.e. comprising a discrete number of stimulation periods. This may be achieved by toggling between a corresponding set of frequency division ratios in the frequency divider 34 as set by the frequency controller 32 under the control of the control unit 23.

To implement the random selection mentioned above, the stimulation periods may be randomly selected from the predetermined set of stimulation periods, i.e. random cycling of the stimulation periods.

Alternatively, the stimulation periods may be dithered with stimulation periods that have lengths varying in a predetermined cycle, i.e. deterministic cycling of the stimulation periods.

In one option, the predetermined cycle comprises different lengths in each period of the stimulation signal, i.e. fast deterministic cycling of the stimulation periods.

In another option, the predetermined cycle comprises the same length in consecutive groups of periods, i.e. slow deterministic cycling of the stimulation periods.

The implementation of dithering by toggling between a predetermined set of stimulation periods will now be discussed.

To ensure that dithered stimulation can be implemented in a broad range of existing stimulation devices, different ways of toggling within a predetermined set of stimulation frequencies (with corresponding stimulation periods) as approximations of white noise based dithered stimulation. Figs. 10A-10C illustrate examples of stimulation signals

generated by toggling between a set of $n$ stimulation frequencies $\{f_{s,1}, f_{s,2}, \ldots, f_{s,n}\}$, with the corresponding stimulation periods symmetrically distributed around the period corresponding to the base stimulation frequency $f_s$, using random cycling, fast deterministic cycling, and slow deterministic cycling, respectively. In the slow deterministic cycling of Fig. 10C, an example is shown where the number $N_r$ of stimulation periods in the consecutive groups is 2, but larger groups could alternatively be used. Exemplar, short stimulation pulses are shown in red, but these approaches can be used for any waveform. Figs. 10B and 10C present two full cycles of the corresponding deterministic cycles.

The simplest way of approximating white noise based dithered stimulation is the random cycling approach illustrated in Fig. 10A. If the stimulation device 1 is unable to generate random numbers, slow deterministic cycling can be implemented by toggling from one stimulation frequency in the set to the next (i.e. from $f_{s,i}$ to $f_{s,i+1}$ for $i = \{1, .., n-1\}$, and from $f_{s,n}$ to $f_{s,1}$) at each stimulation period as shown in Fig. 10B. If the device is unable to toggle between frequencies at each stimulation period, slow deterministic cycling with slower toggling can be implemented as shown for $N_r = 2$ in Fig. 10C.

Given a large enough set of stimulation frequencies, these toggling approaches can achieve selective entrainment in populations of coupled neural oscillators. For simplicity, the distribution of frequencies picked in this analysis correspond to a uniform distribution of stimulation periods, and the frequency sets used are detailed in Fig. 11 as follows.

Fig. 11 shows that selective entrainment can be achieved in populations of coupled neural oscillators by toggling within a finite set of stimulation frequencies. Each row corresponds to a particular type of pulse train, as indicated on the left side of the figure. For slow deterministic cycling (last row), Nr = 3. Fig. 10A shows frequency locking regions in the natural frequency/stimulation amplitude space. Only regions of frequency-locking (determined as presented in the Methods Section below) are shown. The graded scale represents the rotation number. Fig. 10B shows the Arnold tongue width as a function of stimulation amplitude. Fig. 10C shows the mean instantaneous frequency (represented by the color scale) in the natural frequency/stimulation amplitude space. In Figs. 10A and 10C, for each natural frequency, stimulation amplitude, and dithering value, the rotation number or mean instantaneous frequency are averaged over 5 repeats, with 400 stimulation pulses per repeat. The stimulation frequency is indicated by a dashed line.

With only three stimulation frequencies, both random and deterministic cycling fail to realize selective entrainment (first and second rows of Fig. 11). With a set of seven stimulation frequencies, higher-order tongues have vanished with both random and deterministic cycling (Figs. A3 and B3, and Figs. A4 and B4, respectively). Fine structures are still visible at high frequency for deterministic cycling when plotting the mean instantaneous network frequency in the natural frequency/stimulation amplitude space (Fig. 11C4). This is much less the case with this frequency set for random cycling (Fig. 11C4), making random cycling preferable for a set of seven stimulation frequencies. However, with a set of 13 stimulation frequencies, this is no longer an issue for deterministic cycling (second-to-last row of Fig. 11C), and even slow deterministic cycling with $\boldsymbol{N_r = 3}$ is effective (last row of Fig, 11).

Fig. 16 shows the efficacy of the stimulation frequency toggling approach is confirmed by PLV analysis in populations of coupled neural oscillators. Each row correspond to a particular type of pulse train, as indicated on the left of the figure. For slow deterministic cycling (last row), $\mathbf{N_r = 3}$. Figs. 16A1-16A6 show frequency locking regions in the natural frequency/stimulation amplitude space. Only regions of frequency-locking (determined as presented in the Methods Section below), are shown. The grading scale represents the rotation number. Figs. 16B1-16B6 show PLV $\mathbf{p}$:1 (color scale) in the natural frequency/stimulation amplitude space. Here, PLV $\mathbf{p}$:1 detects 1:1 and 2:1 entrainment. Figs. 16C1-16C6 show PLV $\mathbf{p}$:2 (color scale) in the natural frequency/stimulation amplitude space. Here, PLV $\mathbf{p}$:2 detects 1:2 and 3:2 entrainment, but also 1:1 and 2:1 entrainment. Figs 16D1-16D6 show PLV $(\mathbf{2p - 1})$:2 (color scale) in the natural frequency/stimulation amplitude space, obtained as PLV $\mathbf{p}$:2 - PLV $\mathbf{p}$:1. Here, PLV $(\mathbf{2p - 1})$:2 detects 1:2 and 3:2 entrainment.

In all panels, for each natural frequency, stimulation amplitude, and dithering value, the rotation number or mean instantaneous frequency is averaged over 5 repeats, with 400 stimulation pulses per repeat. The stimulation frequency is indicated by dashed lines.

In summary, in populations of coupled neural oscillators, random cycling can achieve selective entrainment with the fewest number of stimulation frequencies. Nevertheless, for devices with more limited capabilities, deterministic cycling and even slow deterministic cycling are effective when a broader set of stimulation frequencies is used.

In general, various forms of distributions of stimulation periods may be used.

The parameters of the distribution of stimulation periods may be selected to provide the selective entrainment.

In one type of example, the stimulation periods may be dithered with a distribution of stimulation periods that is symmetric, for example a uniform distribution (i.e. a rectangular distribution) or a non-uniform distribution, for example a normal distribution or a triangular distribution.

In another type of example, the stimulation periods may be dithered with a distribution of stimulation periods that is asymmetric. In this case, the distribution may have a value of Fisher's moment coefficient of skewness that is 0.2 or less. Fisher's moment coefficient of skewness is given by the equation:

$$\tilde{\mu}_3 = \mathrm{E}\left[\left(\frac{X-\mu}{\sigma}\right)^3\right] = \frac{\mu_3}{\sigma^3} = \frac{\mathrm{E}[(X-\mu)^3]}{(\mathrm{E}[(X-\mu)^2])^{3/2}} = \frac{\kappa_3}{\kappa_2^{3/2}}$$

where $\mu$ is the mean, $\sigma$ is the standard deviation, E is the expectation operator, $\mu_3$ is the third central moment, and $\kappa t$ are the t-th cumulants. It is sometimes referred to as Pearson's moment coefficient of skewness.

The size of the distribution as represented by its standard deviation may similarly be selected to provide the selective entrainment.

In an example applicable to any form of distribution, the distribution may have a standard deviation of 0.5•Tavg or less, preferably $\sqrt{(1/12)}$ •Tavg or less, or more preferably 0.2•Tavg or less, where Tavg is the average length of the periods in the distribution.

In another example applicable to a uniform distribution, the distribution may have values in a range from 0.5.Tavg to 1.5Tavg, where Tavg is the average length of the periods in the distribution (which corresponds to standard deviation of $\sqrt{(1/12)}$ •Tavg or less).

The amplitude of the stimulation signal and/or one or more parameters of the dithering of the stimulation periods of the stimulation signal are selected to obtain entrainment of the target neural rhythm at a target level while maintaining entrainment of the other neural rhythms below a predetermined limit. Such a selection may be performed in advance of operating the stimulation device 1. The reduced entrainment of the other neural rhythms may effectively allow use of a higher amplitude of the stimulation signal than could otherwise be used.

Alternatively, the control unit 23 may adjust the stimulation signal during operation of the stimulation device 1 in response the LPF signal measured by the monitor electrodes

4 and/or in response to the feedback signal from the sensor 5.

As an illustration of this, Fig. 5 is a flow chart of a method of adjusting the stimulation signal generated by the stimulation device of Fig. 1. This method is performed in the control unit 23.

In step S4, the control unit 23 receives a feedback signal, which may be the LFP signal representing neural rhythms of the subject 10, the feedback signal from the sensor 5 (or plural sensors 5, if provided) representing measurements from the subject 10, or a combination thereof.

In step S5, the control unit 23 adjusts the stimulation signal in response to the feedback signal.

The adjustment may be performed to obtain entrainment of the target neural rhythm at a target level while maintaining entrainment of the other neural rhythms below a predetermined limit.

The adjustment of the stimulation signal may be an adjustment of the amplitude of the stimulation signal and/or one or more parameters of the dithering of the stimulation periods of the stimulation signal. In the latter case, the one or more parameters may include the standard deviation of the distribution of the stimulation periods.

The stimulation device 1 may periodically record and store intrinsic neural rhythms, as measured by the LFP signal. These neural rhythms may be associated with physiological or pathological states based on patient feedback and information from other sensors collected throughout the day. Thus, using these adjustment techniques, the stimulation device 1 may provide patient-specific therapy by entraining a neural rhythm identified as physiological and by making sure rhythms identified as pathological are not entrained. This goal can be achieved using selective entrainment based on dithering.

The stimulation frequency may be adjusted to the frequency of the physiological rhythm to entrain.

The stimulation amplitude may be adjusted to obtain a satisfactory therapeutic effect (from entraining the physiological rhythm).

The variability in the stimulation period (parametrised for example by the standard deviation of the distribution of stimulation periods) may be adjusted to make sure entrainment of pathological rhythms is kept below an acceptable level.

Such adjustments could be made periodically during use of the stimulation, typically throughout the day.

In the embodiment discussed above, the target neural rhythm occurs in the brain 14

of the subject 10 and so may be referred to as a brain rhythm. However, in general the present techniques may be adapted to a target neural rhythm occurring in any part of the nervous system as similar principles apply.

In the embodiment discussed above, DBS is used as the stimulation, which is an example of electrical stimulation applied to the brain 14 of the subject. However, the present techniques may be adapted to any form of neural stimulation applied to any part of the nervous system of the subject 10 associated with the target neural rhythm. That may be the same or different physical location within the nervous system of the subject 10. Some non-limitative examples are as follows.

The present techniques have particular applicability to electromagnetic stimulation.

One example of electromagnetic stimulation is electrical stimulation, in which case the stimulation transducer may be an electrode. DBS is an examples of electrical stimulation, but another example is transcranial electrical stimulation, e.g. using electrodes that are located externally of the subject or implanted subdurally.

Another example of electromagnetic stimulation is magnetic stimulation, in which case the stimulation transducer may be an coil. Examples of magnetic stimulation include transcranial magnetic stimulation, e.g. using external coils.

Other types of neural stimulation include acoustic stimulation, in which case the stimulation transducer may be an acoustic transducer, or optical stimulation, in which case the stimulation transducer may be an optical transducer. For example, the present techniques may be applied to non-invasive senosry stimulation, which may for example be used to treat Alzheimer's disease.

As in the above embodiment, the neural stimulation signal may be applied to the brain of the subject, but in general the neural stimulation signal may be applied to any part of the nervous system as similar principles apply. The neural stimulation signal may be applied to a part of the nervous system of the subject.

While the example above uses the LFP signal as the electrophysiological signal representing neural rhythms of the subject, other types of electrophysiological signal may be used. One example of an alternative type of electrophysiological signal is an electroencephalography (EEG) signal in which case the monitor transducer may be electrodes that are located externally of the subject or implanted subdurally.

The target neural rhythm occurs in the nervous system of the subject. Often the target neural rhythm may occur in the brain of the subject, but in general the target neural rhythm may occur in any part of the nervous system as similar principles apply.

Methods Section

In this section, there is approximated analytically the width of Arnold tongue families in the presence of dithered stimulation, and provided methodological details pertaining to entrainment metrics and to the simulation of networks of coupled neural oscillators.

The theoretical basis for the efficacy of dithered stimulation as a selective entrainment strategy is as follows.

By deriving approximate expressions for the width of the most prominent families of Arnold tongues as a function of the dithering level, a theoretical basis for the efficacy of dithered stimulation is proposed as a selective entrainment strategy.

The influence of dithered stimulation on p:1 Arnold tongues is as follows.

Cobweb plots are considered to study the $p$:1 frequency locking behavior of the stochastic sine circle map given by equation (2), for $p \geq 1$. In the deterministic case, $p$:1 frequency locking corresponds to the stable fixed point of $\theta_{n+1} = F(\theta_n)$ and $\theta_{n+1} = \theta_n + 2p\pi$, i.e. when there are $p$ complete rotations of the oscillator for every stimulation cycle.

Fig. 12 shows cobweb plots of the deterministic sine circle map for different frequency locking ratios. Cobweb plots used to study frequency-locking in the deterministic sine circle map reveal the size of the trap (denoted by $h$, shortest distance between a stable and an unstable fixed point) that can prevent dithered stimulation from breaking frequency locking. Stable fixed points are identified by filled red circles, unstable fixed points by empty red circles.

The cobweb plot representing $\theta_{n+1}$ as a function of $\theta_n$ has one stable and one unstable fixed points (see Fig. 12A for the 1:1 case and Fig. 12B for the 1:2 case). In the stochastic case, there will still be $p$:1 frequency locking if it is highly unlikely for the phase to escape the attraction "trap" between the stable and unstable fixed points in one random jump [43] (i.e. after one iteration of the stochastic map). $h$ denotes the size of the trap as indicated in Fig. 12A-12B.

The random jump size (mod $\boldsymbol{2\pi}$) between stimulation pulse $\boldsymbol{n}$ and $\boldsymbol{n+1}$ is $\boldsymbol{\theta_{n+1} - \theta_n \approx 2\pi(f_0/f_s)z_n}$ since $\boldsymbol{\theta_n \approx F(\theta_n) \bmod 2\pi}$ in the vicinity of the stable fixed point. Therefore the jump size is approximately distributed according to $\boldsymbol{\mathcal{N}(0, \sigma^2)}$ with $\boldsymbol{\sigma = 2\pi(f_0/f_s)\zeta}$. It is considered highly unlikely for the phase to clear the trap if the trap size $\boldsymbol{h}$ is larger than $\boldsymbol{n_\sigma}$ standard deviations of the jump size distribution, with $\boldsymbol{n_\sigma \geq 3}$. In [43], $\boldsymbol{n_\sigma = 3}$, but $\boldsymbol{n_\sigma \geq 3}$ is considered for the sake of generality. Therefore, frequency locking

is lost when:

$$\boldsymbol{h = 2\pi(f_0/f_s)n_\sigma\zeta} \quad (5)$$

The trap size $\boldsymbol{h}$ can be obtained by solving for the positions of the stable and unstable fixed points of the deterministic map, and selecting the shortest absolute distance between the fixed points. For the $\boldsymbol{p}$:1 case:

$$\boldsymbol{h} = \begin{cases} \boldsymbol{\pi + 2\arcsin\left(\frac{2\pi}{I}\left[\frac{f_0}{f_s} - p\right]\right)} & \text{for } \boldsymbol{\frac{f_0}{f_s} < p} \\ \boldsymbol{\pi - 2\arcsin\left(\frac{2\pi}{I}\left[\frac{f_0}{f_s} - p\right]\right)} & \text{for } \boldsymbol{\frac{f_0}{f_s} > p} \end{cases}$$

Using this result and equation (5), the $p$:1 tongue boundaries of the stochastic sine circle map are obtained as:

$$\boldsymbol{I(f_0) = \frac{\pm 2\pi\left(\frac{f_0}{f_s} - p\right)}{\sin\left(\pi\left[\frac{f_0}{f_s}n_\sigma\zeta - \frac{1}{2}\right]\right)}} \quad (6)$$

Under the assumption that the standard deviation of the noise is small ($\zeta \ll 1$), the width of the p:1 tongue can be approximated. This requires finding the function $f_0^+(I)$ demarcating the right boundary of the tongue and the function $f_0^-(I)$ demarcating the left boundary. At the right boundary of the tongue ($f_0^+/f_s > p$), a Taylor expansion of the sine term in equation (6) to second order in $\zeta$ gives the quadratic equation:

$$\boldsymbol{\frac{\pi^2}{2}n_\sigma^2\zeta^2 I\left(\frac{f_0^+}{f_s}\right)^2 + 2\pi\frac{f_0^+}{f_s} - (2p\pi + I) = 0}$$

which, after a Taylor expansion to second order in $\zeta$ of the square root of the quadratic equation discriminant, yields:

$$\boldsymbol{f_0^+(I) = f_s\left(p + \frac{I}{2\pi} - \frac{n_\sigma^2\zeta^2}{16\pi}I[2p\pi + I]^2\right)}$$

Similarly, for the left boundary of the tongue:

$$\boldsymbol{f_0^-(I) = f_s\left(p - \frac{I}{2\pi} + \frac{n_\sigma^2\zeta^2}{16\pi}I[2p\pi - I]^2\right)}$$

Thus, the width of $p$:1 Arnold tongues can be approximated in the stochastic sine circle map as:

$$\boldsymbol{\Delta f^{p:1}(I) = f_0^+(I) - f_0^-(I) = f_s\frac{I}{\pi}\left(1 - \frac{n_\sigma^2\zeta^2}{8}[4p^2\pi^2 + I^2]\right)} \quad (7)$$

The influence of dithered stimulation on (2p-1):2 Arnold tongues is as follows.

In the sine circle map, Arnold tongues of order $(2p-1)$:2, $p \geq 1$, are the second

largest after tongues of order $p$:1 (Fig. 8A1). Their widths can be approximated by adapting the derivation presented in the previous section. In the deterministic case, $(2p-1)$:2 frequency locking is characterised by $2p-1$ complete rotations of the oscillator for every two stimulation cycles. Since two stimulation cycles are considered, $(2p-1)$:2 frequency locking corresponds to stable fixed points of the map given by equation (1) iterated twice, i.e. $\theta_{n+2} = F\big(F(\theta_n)\big)$, and $\theta_{n+2} = \theta_n + 2(2p-1)\pi$. The random jump size between stimulation pulse $n$ and $n+2$ is:

$$\begin{aligned}\boldsymbol{\theta_{n+2} - \theta_n} &= \boldsymbol{F\left(F(\theta_n) + 2\pi\frac{f_0}{f_s}z_n\right) + 2\pi\frac{f_0}{f_s}z_{n+1} - \theta_n}\\ \boldsymbol{\theta_{n+2} - \theta_n} &\approx \boldsymbol{F\big(F(\theta_n)\big) + 2\pi\frac{f_0}{f_s}z_n\big(1 + I\cos F(\theta_n)\big) + 2\pi\frac{f_0}{f_s}z_{n+1} - \theta_n}\end{aligned}$$

where a Taylor expansion is used to first order (assuming that $\zeta \ll 1$). Assuming $I \ll 1$, and since $\theta_n \approx F\big(F(\theta_n)\big) \bmod 2\pi$ in the vicinity of the stable fixed points, $\theta_{n+2} - \theta_n \approx 2\pi(f_0/f_s)(z_n + z_{n+1}) \bmod 2\pi$. Therefore the jump size is approximately distributed according to $\mathcal{N}(0, \sigma^2)$ with $\sigma = 2\sqrt{2}\pi(f_0/f_s)\zeta$.

As before, the shortest trap size $\boldsymbol{h}$ is obtained by solving for the position of the stable and unstable fixed points of the deterministic map (see Fig. 12 C-D for the 1:2 and 3:2 case, respectively). Iterating the deterministic map twice gives:

$$\boldsymbol{\theta_{n+2} = \theta_n + 4\pi\frac{f_0}{f_s} + I\left(\sin\theta_n + \sin\left[\theta_n + 2\pi\frac{f_0}{f_s} + I\sin\theta_n\right]\right).}$$

If $f_0$ is close to the center of the $(2p-1)$:2 tongue, $\delta = (f_0/f_s) - (2p-1)/2$ is small. Assuming $I \ll 1$ and $\delta \ll I$ yields:

$$\begin{aligned}\boldsymbol{\theta_{n+2}} &= \boldsymbol{\theta_n + 4\pi\frac{f_0}{f_s} + I\left\{\sin\theta_n + \sin\left(\theta_n + 2\pi\left[\delta + \frac{2p-1}{2}\right] + I\sin\theta_n\right)\right\},}\\ \boldsymbol{\theta_{n+2}} &\approx \boldsymbol{\theta_n + 4\pi\frac{f_0}{f_s} - \frac{I^2}{2}\sin(2\theta_n)} \qquad \textbf{(8)}\end{aligned}$$

Thus, when $(2p-1)$:2 frequency locking occurs, there are four fixed points which satisfy:

$$\boldsymbol{4\pi\left(\frac{f_0}{f_s} - \frac{2p-1}{2}\right) - \frac{I^2}{2}\sin(2\theta_n) \approx 0.}$$

It is noted that when using equation (8), since the distances between each stable fixed point and the nearest unstable fixed point are the same (see Fig. 12C-D), it does not matter at which stable fixed point locking occurs. The trap size $h$ is therefore obtained by selecting the shortest distance between one of the stable fixed points and an unstable fixed point. For the $(2p-1)$:2 case:

$$h \approx \begin{cases} \frac{\pi}{2} + \arcsin\left(\frac{8\pi\left[\frac{f_0}{f_s} - \frac{2p-1}{2}\right]}{I^2}\right) & \text{for } \frac{f_0}{f_s} < p \\ \frac{\pi}{2} - \arcsin\left(\frac{8\pi\left[\frac{f_0}{f_s} - \frac{2p-1}{2}\right]}{I^2}\right) & \text{for } \frac{f_0}{f_s} > p \end{cases}$$

Boundaries for $(2p-1)$:2 tongues in the stochastic sine circle map are obtained from the condition $h = n_\sigma \sigma$, which translates to:

$$I(f_0) = \left(\pm \frac{8\pi\left[\frac{f_0}{f_s} - \frac{2p-1}{2}\right]}{\sin\left\{\pi\left[2\sqrt{2}\frac{f_0}{f_s} n_\sigma \zeta - \frac{1}{2}\right]\right\}}\right)^{1/2} \qquad (9)$$

As in the $p$:1 case, the width of $(2p-1)$:2 tongues can be approximated by inverting equation (9) to find the functions $f_0^+(I)$ at the right boundary, and $f_0^-(I)$ at the left boundary. At the right boundary of the tongue ($f_0^+/f_s > (2p-1)/2$), a Taylor expansion of the sine term in equation (9) to second order in $\zeta$ give the quadratic equation:

$$4\pi^2 n_\sigma^2 \zeta^2 I^2 \left(\frac{f_0^+}{f_s}\right)^2 + 8\pi \frac{f_0^+}{f_s} - (4\{2p-1\}\pi + I^2) = 0$$

which, after a Taylor expansion to second order in $\zeta$ of the square root of the quadratic equation discriminant, yields:

$$f_0^+(I) = f_s\left(\frac{2p-1}{2} + \frac{I^2}{8\pi} - \frac{n_\sigma^2 \zeta^2}{128\pi} I^2 [4\{2p-1\}\pi + I^2]^2\right)$$

Similarly, for the left boundary of the tongue:

$$f_0^-(I) = f_s\left(\frac{2p-1}{2} - \frac{I^2}{8\pi} + \frac{n_\sigma^2 \zeta^2}{128\pi} I^2 [4\{2p-1\}\pi - I^2]^2\right)$$

Thus, the width of $(2p-1)$:2 Arnold tongues can be approximated in the stochastic sine circle map as:

$$\Delta f^{(2p-1):2}(I) = f_0^+(I) - f_0^-(I) = f_s \frac{I^2}{4\pi}\left(1 - \frac{n_\sigma^2 \zeta^2}{16}[16\{2p-1\}^2\pi^2 + I^4]\right) \qquad (10)$$

Entrainment metrics used in simulations are as follows.

Several entrainment metrics are computed to characterise the frequency locking behavior of neural oscillators in simulations. The primary entrainment metric, the rotation number $R$, is measured as:

$$R = \frac{\phi_N - \phi_0}{2\pi N},$$

where $N$ is large, and $\phi_n$ is specified depending on the model considered. In simulations of the sine circle map, taking $\phi_n = \theta_n$. In simulations of the Kuramoto model, using $\phi_n = \psi(t_n)$ where $\psi(t)$ is the phase of the order parameter $\mathcal{Z}(t)$ (see definitions below), and $t_n$ is the time one time step before stimulation pulse $n$. For reference, theoretical definitions of the rotation number in the presence of stochasticity are given in [58, 52].

To detect frequency locking in the presence of noise, the following criterion is used for both models. The system is considered to be entrained to stimulation with a $\boldsymbol{p}$:$\boldsymbol{q}$ rotation number if $|\boldsymbol{R} - \boldsymbol{p}/\boldsymbol{q}| <$ tol, and $|\boldsymbol{S}(\boldsymbol{\partial R}/\boldsymbol{\partial f_0})| <$ tol$'$, where $\boldsymbol{S}(\boldsymbol{\partial R}/\boldsymbol{\partial f_0})$ is the smoothed partial derivative of the measured rotation number with respect to $\boldsymbol{f_0}$, and tol and tol$'$ are tolerances on the rotation number and its smoothed derivative, respectively. These conditions correspond to plateaux in Fig. 7 where $\boldsymbol{p}$:$\boldsymbol{q}$ frequency locking occurs. For simulations of the sine circle map, taking tol $= \boldsymbol{6.10^{-4}}$, tol$' = \boldsymbol{1.10^{-2}}$, and $\boldsymbol{\partial R}/\boldsymbol{\partial f_0}$ is smoothed using locally weighted scatterplot smoothing (LOWESS, based on a linear model) with a span of 0.058 Hz (4 samples). For simulations in the Kuramoto model, taking tol $= \boldsymbol{3.10^{-2}}$, tol$' = \boldsymbol{2.10^{-2}}$, and $\boldsymbol{\partial R}/\boldsymbol{\partial f_0}$ is smoothed using LOWESS with a span of 0.64 Hz (4 samples). These values take into account the different resolutions of the rotation number field for both models in the natural frequency/stimulation amplitude space, simulation duration, and simulation repeats, and were found to robustly detect frequency locking plateaux.

For both models, the width of the $\boldsymbol{p}$:$\boldsymbol{q}$ tongue for a particular stimulation amplitude and dithering level is simply measured in simulations as the sum of the frequency width of the discretised bins in the natural frequency/stimulation amplitude space where $\boldsymbol{p}$:$\boldsymbol{q}$ entrainment is detected at this stimulation amplitude and dithering level.

Additionally, the mean instantaneous frequency in the Kuramoto model is computed as:

$$\boldsymbol{f}_{\text{inst}} = \left\langle \frac{\mathbf{1}}{\boldsymbol{2\pi}} \frac{\mathbf{d}\boldsymbol{\psi}}{\mathbf{d}\boldsymbol{t}} \right\rangle,$$

where $\psi$ is the phase of the order parameter (see definitions below), and $\langle . \rangle$ denotes the time average over the duration of stimulation.

Populations of coupled neural oscillators may be simulated as follows.

In order to test dithered stimulation in populations of coupled neural oscillators, $M = 100$ coupled Kuramoto oscillators were simulated with noise and homogeneous coupling. The time evolution of the phase $\varphi_k$ of the $k^{\text{th}}$ oscillator is described by the stochastic differential equation:

$$\mathbf{d}\boldsymbol{\varphi}_k = \left[\boldsymbol{\omega}_k + \frac{\boldsymbol{\kappa}}{\boldsymbol{M}}\sum_{\boldsymbol{l=1}}^{\boldsymbol{M}} \mathbf{sin}\left(\boldsymbol{\varphi}_k - \boldsymbol{\varphi}_l\right) + \boldsymbol{I}(\boldsymbol{t})\boldsymbol{Z}(\boldsymbol{\varphi}_k)\right]\mathbf{d}\boldsymbol{t} + \boldsymbol{\xi}\mathbf{d}\boldsymbol{W}_k$$

where $\omega_k$ is the intrinsic frequency of the $k^{\text{th}}$ oscillator, $\kappa$ is the coupling strength, $I(t)$ is the stimulation pulse train, $Z$ is the oscillator PRC, and $W_k$ are independent Wiener processes. The order parameter of the network reads $\mathcal{Z}(t) = \Sigma_{k=1}^{M} e^{i\varphi_k(t)}/M = \rho(t)e^{i\psi(t)}$. A more computationally efficient form of equation (11), involving the modulus $\rho$ and phase $\psi$ of the order parameter, is given by:

$$\mathbf{d}\boldsymbol{\varphi}_k = [\boldsymbol{\omega}_k + \boldsymbol{\kappa}\boldsymbol{\rho}\mathbf{sin}(\boldsymbol{\psi} - \boldsymbol{\varphi}_k) + \boldsymbol{I}(\boldsymbol{t})\boldsymbol{Z}(\boldsymbol{\varphi}_k)]\mathbf{d}\boldsymbol{t} + \boldsymbol{\xi}\mathbf{d}\boldsymbol{W}_k.$$

Signals with dynamics similar to neural oscillations in the absence of stimulation were reproduced by choosing $\kappa = 350$, $\xi = 7.9$, and sampling the $\omega_k$'s from a Lorentzian distribution centered on the frequency considered ($f_0/[2\pi]$) and of width 20 Hz. Examples of output signals $\mathcal{X}(t) = \Re\big(\mathcal{Z}(t)\big)$ [44], where $\Re$, are shown in Fig. 17A for two values of $f_0$. Taking $Z$ to be the PRC of the standard Hodgkin-Huxley neuron model [48, 49], see Fig. 17B1. In Fig. 9 and Fig. 15, the dithered stimulation pulse train $I(t)$ is constructed with its stimulation period changing at each stimulation period and given by $(1 + z)/f_s$, where $f_s = 130$ Hz is the base stimulation frequency, and $z$ is a normal random number sampled from $\mathcal{N}(0, \zeta^2)$ at each stimulation period. In Fig. 11 and Fig. 16, the stimulation pulse train is constructed as described therein using a finite set of stimulation frequencies. In both cases, contrary to the sine circle map, square stimulation pulses are considered with a temporal extent, as shown in Fig. 17B2. The positive stimulation pulse is taken to be 20% of the stimulation period. To avoid harming the brain, charge balance is also enforced, and a negative stimulation pulse occupies the rest of the stimulation period. The magnitude of the positive component is chosen so that the time integral of the stimulation waveform over a period is zero. The model is forward simulated using a Euler-Maruyama scheme with a time step of $10^{-4}$ s.

References

[2] Doelling et al. An oscillator model better predicts cortical entrainment to music. Proceedings of the National Academy of Sciences of the United States of America, 116(20):10113–10121, 2019. doi:10.1073/pnas.1816414116.

[3] Herrmann et al. Human EEG responses to 1-100 Hz flicker Resonance phenomena in visual cortex and their potential correlation to cognitive phenomena. Experimental Brain Research, 137(3-4):346–353, 2001. doi:10.1007/s002210100682.

[4] Notbohmet al. Modification of brain oscillations via rhythmic light stimulation

provides evidence for entrainment but not for superposition of event-related responses. Frontiers in Human Neuroscience, 10(FEB2016), 2016. doi:10.3389/fnhum.2016.00010.

[6] Lowet et al. A quantitative theory of gamma synchronization in macaque V1. eLife, 6, 2017. doi:10.7554/eLife.26642.001.

[11] Fröhlich. Tuning out the blues – Thalamo-cortical rhythms as a successful target for treating depression, nov 2015. doi:10.1016/j.brs.2015.07.040.

[13] Ozen et al. Transcranial electric stimulation entrains cortical neuronal populations in rats. Journal of Neuroscience, 30(34):11476–11485, aug 2010. doi:10.1523/JNEUROSCI.5252-09.2010.

[14] Johnson et al. Dose-dependent effects of transcranial alternating current stimulation on spike timing in awake nonhuman primates. Science Advances, 6(36), sep 2020. doi:10.1126/sciadv.aaz2747.

[15] Krause et al.. Transcranial alternating current stimulation entrains single-neuron activity in the primate brain. Proceedings of the National Academy of Sciences of theUnited States of America, 116(12):5747–5755, 2019. doi:10.1073/pnas.1815958116.

[16] Cleary et al. Deep brain stimulation entrains local neuronal firing in human globus pallidus internus. Journal of Neurophysiology, 109(4):978–987, feb 2013. doi:10.1152/jn.00420.2012.

[17] Leuchter et al. Efficacy and safety of low field synchronized transcranial magnetic stimulation (sTMS) for treatment of major depression. Brain Stimulation, 8(4):787–794, jul 2015. doi:10.1016/j.brs.2015.05.005.

[18] Ahn et al. . Identifying and Engaging Neuronal Oscillations by Transcranial Alternating Current Stimulation in Patients With Chronic Low Back Pain: A randomized, Crossover, Double-Blind, Sham-Controlled Pilot Study. Journal of Pain, 20(3):277.e1–277.e11, mar 2019. doi:10.1016/j.jpain.2018.09.004.

[19] Iaccarino et al. Gamma frequency entrainment attenuates amyloid load and modifies microglia. Nature, 540(7632):230–235, dec 2016. doi:10.1038/nature20587.

[20] Martorell et al.. Multi-sensory Gamma Stimulation Ameliorates Alzheimer's-Associated Pathology and Improves Cognition. Cell, 177(2):256–271.e22, 2019. doi:10.1016/j.cell.2019.02.014.

[21] Chan et al. 40Hz sensory stimulation induces gamma entrainment and affects brain structure, sleep and cognition in patients with Alzheimer's dementia. medRxiv, 15(6):17, 2021. doi:10.1101/2021.03.01.21252717.

[22] Fischer et al. Entraining stepping movements of Parkinson's patients to alternating

subthalamic nucleus deep brain stimulation. Journal of Neuroscience, 40(46):8964–8972, 2020. doi:10.1523/JNEUROSCI.1767-20.2020.

[23] Guerra et al. Driving motor cortex oscillations modulates bradykinesia in Parkinson's disease. Brain, page awab257, Jul 2021. doi:10.1093/brain/awab257.

[24] Wiest et al. Finely-tuned gamma oscillations: Spectral characteristics and links to dyskinesia. Experimental Neurology, 351:113999, may 2022. doi:10.1016/j.expneurol.2022.113999.

[25] Swann et al. Gamma oscillations in the hyperkinetic state detected with chronic human brain recordings in Parkinson's disease. Journal of Neuroscience, 36(24):6445–6458, 2016. doi:10.1523/JNEUROSCI.1128-16.2016.

[26] Swann et al. Adaptive deep brain stimulation for Parkinson's disease using motor cortex sensing. Journal of Neural Engineering, 15(4):046006, May 2018. doi:10.1088/1741-2552/aabc9b.

[27] Sermon et al.. Sub-harmonic Entrainment of Cortical Gamma Oscillations to Deep Brain Stimulation in Parkinson's Disease: Predictions and Validation of a Patient-Specific Non-Linear Model. bioRxiv, page 2022.03.01.482549, Mar 2022. doi:10.1101/2022.03.01.482549.

[28] Zamora et al. Case Report: Embedding "Digital Chronotherapy" Into Medical Devices—A Canine Validation for Controlling Status Epilepticus Through Multi-Scale Rhythmic Brain Stimulation. Frontiers in Neuroscience, 15:1196, Sep 2021. doi:10.3389/fnins.2021.734265.

[29] Frohlich et al. Brainwave entrainment for the treatment of chronic pain: comment on Br J Pain 2020; 14: 161–70, Mar 2021. doi:10.1177/2049463721994614.

[30] Pikovsky et al. Synchronization: A Universal Concept in Nonlinear Sciences. Cambridge University Press, Oct 2001. doi:10.1017/CBO9780511755743.

[31] Lysyansky et al. Multi-frequency activation of neuronal networks by coordinated reset stimulation. Interface Focus, 1(1):75–85, 2011. doi:10.1098/rsfs.2010.0010.

[32] Roberts et al. Quantitative theory of driven nonlinear brain dynamics. NeuroImage, 62(3):1947–1955, 2012. doi:10.1016/j.neuroimage.2012. 05.054.

[33] Wilson et al. Clustered Desynchronization from High-Frequency Deep Brain Stimulation. PLoS Computational Biology, 11(12):e1004673, 2015. doi: 10.1371/journal.pcbi.1004673.

[34] Herrmann,et al. Shaping intrinsic neural oscillations with periodic stimulation. Journal of Neuroscience, 36(19):5328–5337, 2016. doi:10.1523/JNEUROSCI.0236-16.2016.

[35] Pérez-Cervera et al. Phase-locked states in oscillating neural networks and their role in neural communication. Communications in Nonlinear Science and Numerical Simulation, 80:104992, 2020. arXiv:1905.06038, doi:10.1016/j.cnsns.2019.104992.

[36] Arnold. Remarks on the perturbation theory for problems of Mathieu type. Russian Mathematical Surveys, 38(4):215–233, 1983. doi:10.1070/rm1983v038n04abeh004210.

[37] Lingnau et al. . Universal generation of devil's staircases near Hopf bifurcations via modulated forcing of nonlinear systems. Physical Review E, 102(3), 2020. doi: 10.1103/PhysRevE.102.030201.

[38] Barnikolet al. Tremor entrainment by patterned low-frequency stimulation. Philosophical Transactions of the Royal Society A: Mathematical, Physical and Engineering Sciences, 366(1880):3545–3573, Oct 2008. doi: 10.1098/rsta.2008.0104.

[43] Borisyuk et al. Quasiperiodicity and phase locking in stochastic circle maps: A spectral approach. Physica D: Nonlinear Phenomena, 288:30–44, 2014. doi:10.1016/j.physd.2014.07.006.

[44] GihanWeerasinghe, Benoit Duchet, Hayriye Cagnan, Peter Brown, Christian Bick, and Rafal Bogacz. Predicting the effect so fdee pbrai nstimulatio nusin g areduce e coupled oscillator model. PLOS Computational Biology, 15(8):e1006575, aug 2019. doi:10.1371/journal.pcbi.1006575.

[45] Phuong Thi Mai Nguyen, Yoshikatsu Hayashi, Murilo Da Silva Baptista, and Toshiyuki Kondo. Collective almost synchronization-based model to extract and predict features of EEG signals. Scientifi cReports 10(1):16342, 2020. doi: 10.1038/s41598-020-73346-z.

[46] Gihan Weerasinghe, Benoit Duchet, Christian Bick, and Rafal Bogacz. Optimal closed-loop deep brain stimulation usingmultiple independently controlled contacts. PLOS Computational Biology, 17(8):e1009281, aug 2021. doi:10.1371/journal. pcbi.1009281.

[47] YoshikiKuramoto. Self-entrainment of apopulationof couplednon-linear oscillators. In International symposium on mathematical problems in theoretical physics, pages 420–422. Springer, 1975.

[48] A. L. Hodgkin and A. F. Huxley. A quantitative description of membrane current and its application to conduction and excitation innerve. The Journal of Physiology, 117(4):500–544, aug 1952. doi:10.1113/jphysiol.1952.sp004764.

[49] Eric Brown, JeffMoehlis and Philip Holmes. On the phase reduction and response

dynamics of neural oscillator populations. Neural Computation, 16(4):673–715, apr 2004. doi:10.1162/089976604322860668.

[50] Huang et al. Transcranial alternating current stimulation entrains alpha oscillations by preferential phase synchronization of fast-spiking cortical neurons to stimulation waveform. Nature Communications, 12(1), 2021. doi:10.1038/s41467-021-23021-2.

[52] Nesse et al. Spike patterning of a stochastic phasemodel neuron given periodic inhibition. Physical Review E - Statistical, Nonlinear, and Soft Matter Physics, 75(3), 2007. doi:10.1103/PhysRevE.75.
031912.

[57] Muthuraman et al. Cross-frequency couplingbetweengamma oscillations anddeepbrain stimulation frequency in Parkinson's disease. Brain : a journal of neurology, 43(11):3393–3407, Nov 2020. doi:10.1093/brain/awaa297.

[58] Yamanobe et al. Response of a pacemaker neuron model to stochastic pulse trains. Biological Cybernetics, 86(2):155–166, 2002. doi:10.1007/s00422-001-0287-9

Claims

1. A stimulation device for selective entrainment of a target neural rhythm of a subject, the stimulation device comprising a stimulation circuit arranged to generate a stimulation signal that is periodic and has stimulation periods that are dithered with an average period corresponding to an entrainment frequency of the target neural rhythm such that neural stimulation using the stimulation signal is capable of causing entrainment of the target neural rhythm at the entrainment frequency and minimising entrainment of other neural rhythms at integer ratios of the entrainment frequency.

2. A stimulation device according to claim 1, wherein the stimulation periods are dithered by toggling between a predetermined set of stimulation periods.

3. A stimulation device according to claim 2, wherein the stimulation periods are dithered with stimulation periods that have lengths varying in a predetermined cycle.

4. A stimulation device according to claim 3, wherein the predetermined cycle comprises different lengths in each period of the stimulation signal.

5. A stimulation device according to claim 3, wherein the predetermined cycle comprises the same length in consecutive groups of periods.

6. A stimulation device according to claim 1 or 2, wherein the stimulation periods are dithered with stimulation periods that are randomly selected from a predetermined distribution of stimulation periods.

7. A stimulation device according to any one of the preceding claims, wherein the stimulation periods are dithered with a distribution of stimulation periods that is symmetric.

8. A stimulation device according to claim 7, wherein the distribution is a uniform distribution.

9. A stimulation device according to claim 7, wherein the distribution is a

non-uniform distribution.

10. A stimulation device according to any one of claims 1 to 6, wherein the stimulation periods are dithered with a distribution of stimulation periods that is asymmetric.

11. A stimulation device according to claim 10, wherein the distribution has a value of Fisher's moment coefficient of skewness that is 0.2 or less.

12. A stimulation device according to any one of the preceding claims, wherein the stimulation periods are dithered with a distribution of stimulation periods that has a standard deviation of 0.5•Tavg or less, preferably $\sqrt{(1/12)}$ •Tavg or less, or more preferably 0.2•Tavg or less, where Tavg is the average length of the periods in the distribution.

13. A stimulation device according to claim 10, wherein the distribution has values in a range from 0.5•Tavg to 1.5•Tavg, where Tavg is the average length of the periods in the distribution.

14. A stimulation device according to any one of the preceding claims, wherein an amplitude of the stimulation signal and/or one or more parameters of the dithering of the stimulation periods of the stimulation signal are selected to obtain entrainment of the target neural rhythm at a target level while maintaining entrainment of the other neural rhythms below a predetermined limit.

15. A stimulation device according to any one of the preceding claims, wherein the device further comprises a control circuit arranged to receive a feedback signal representing measurements from the subject and to adjust the stimulation signal in response to the feedback signal.

16. A stimulation device according to claim 15, wherein the feedback signal is an electrophysiological signal representing neural rhythms of the subject.

17. A stimulation device according to claim 15 or 16, wherein the control circuit is arranged to adjust the stimulation signal to obtain entrainment of the target neural rhythm at a target level while maintaining entrainment of the other neural rhythms below a

predetermined limit.

18. A stimulation device according to any one of claims 15 to 17, wherein the adjustment of the stimulation signal is adjustment of an amplitude of the stimulation signal and/or one or more parameters of the dithering of the stimulation periods of the stimulation signal.

19. A stimulation device according to claim 18, wherein the one or more parameters of the dithering of the stimulation periods of the stimulation signal include the standard deviation of the distribution of the stimulation periods.

20. A stimulation device according to any one of the preceding claims, wherein the device further comprises a monitor transducer arranged to measure the electrophysiological signal representing neural rhythms of the subject.

21. A stimulation device according to any one of the preceding claims, wherein the stimulation signal comprises stimulation pulses.

22. A stimulation device according to any one of the preceding claims, wherein the stimulation device further comprises a stimulation transducer arranged to receive the stimulation signal for applying the stimulation signal to the nervous system of the subject.

23. A stimulation device according to any one of the preceding claims, wherein the target neural rhythm is a neural rhythm for treatment of a neurological disorder.

24. A stimulation device according to any one of the preceding claims, wherein the neural stimulation is electromagnetic stimulation.

25. A stimulation device according to claim 24, wherein the electromagnetic stimulation is deep brain stimulation.

26. A method of operating a neural stimulation device for selective entrainment of a target neural rhythm of a subject, the method comprising causing a stimulation circuit to generate a stimulation signal that is periodic and has stimulation periods that are dithered

with an average period corresponding to an entrainment frequency of the target neural rhythm such that neural stimulation using the stimulation signal is capable of causing entrainment of the target neural rhythm at the entrainment frequency and minimising entrainment of other neural rhythms at integer ratios of the entrainment frequency.

27. A method according to claim 26, wherein the method further comprises:

receiving a feedback signal representing measurements from the subject; and

adjusting the stimulation signal in response to the feedback signal.

28. A method according to claim 26 or 27, wherein the feedback signal is an electrophysiological signal representing neural rhythms of the subject.

29. A method according to claim 28, wherein the step of adjusting the stimulation signal is performed to obtain entrainment of the target neural rhythm at a target level while maintaining entrainment of the other neural rhythms below a predetermined limit.

30. A method according to any one of claims 27 to 29, wherein the adjustment of the stimulation signal is adjustment of an amplitude of the stimulation signal and/or parameters of the dithering of the stimulation periods of the stimulation signal.

31. A method according to claim 30, wherein the one or more parameters of the dithering of the stimulation periods of the stimulation signal include the standard deviation of the distribution of the stimulation periods.

32. A method of treatment of a neurological disorder of a subject, the method comprising:

selecting a target neural rhythm for treatment of the neurological disorder;

performing a method of operating a stimulation device according to any one of claims 1 to 25 for entrainment of the target neural rhythm; and

applying the stimulation signal to the nervous system of the subject.

Fig. 1

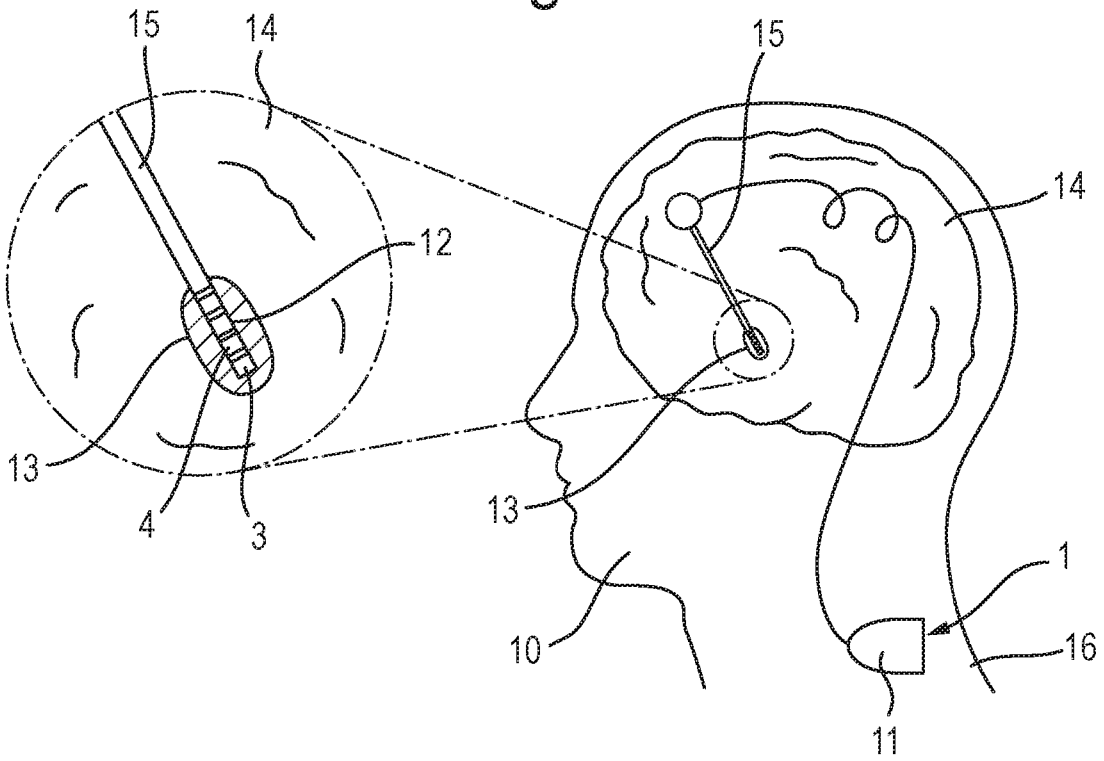
15
14
15
14
12
13
4
3
13
1
10
16
11

Fig. 2

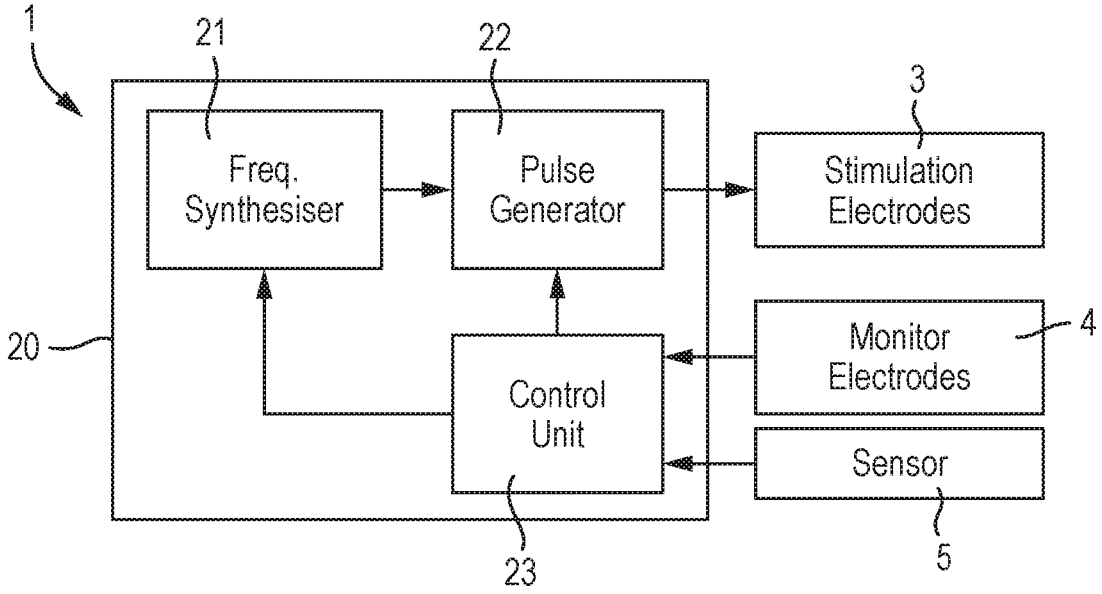
1
21
22
3
Freq. Synthesiser
Pulse Generator
Stimulation Electrodes
20
Monitor Electrodes
4
Control Unit
Sensor
23
5

Fig. 3

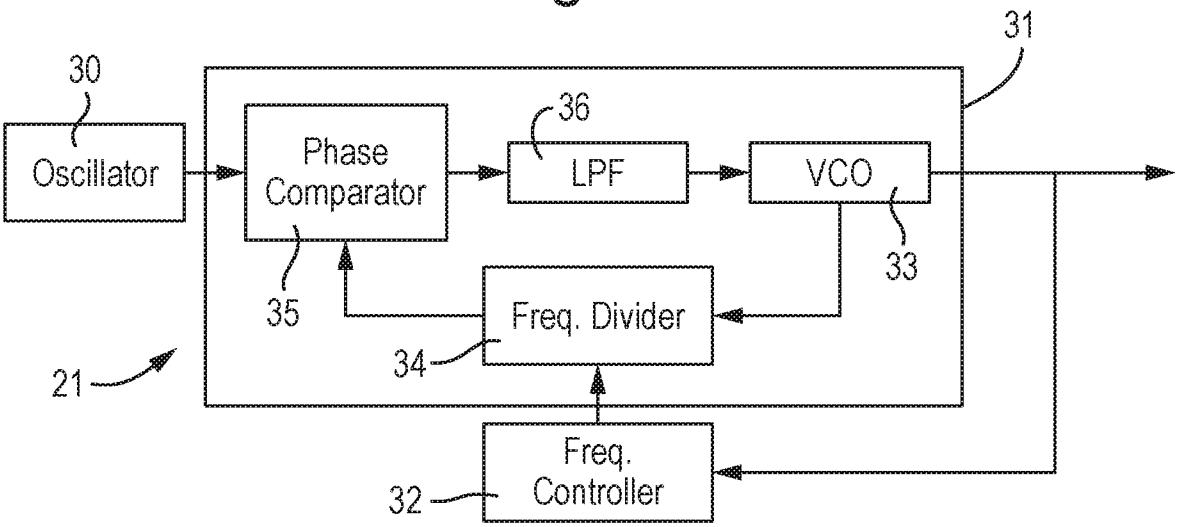


Fig. 4

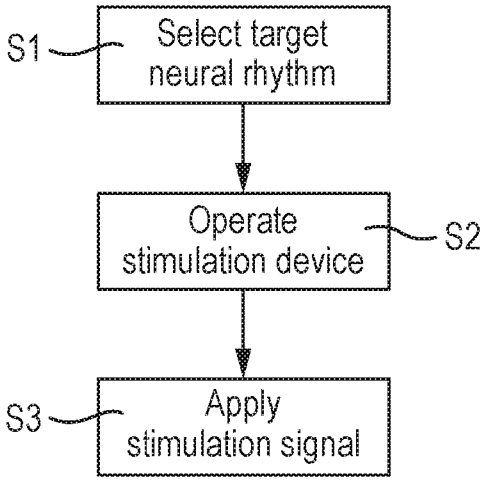


Fig. 5

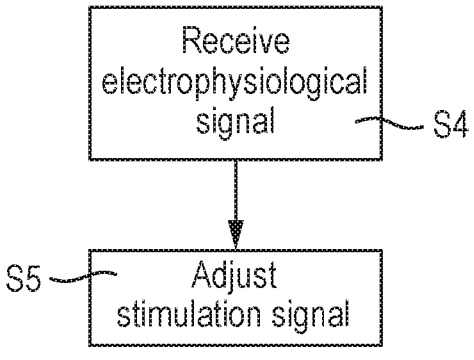

Fig. 6

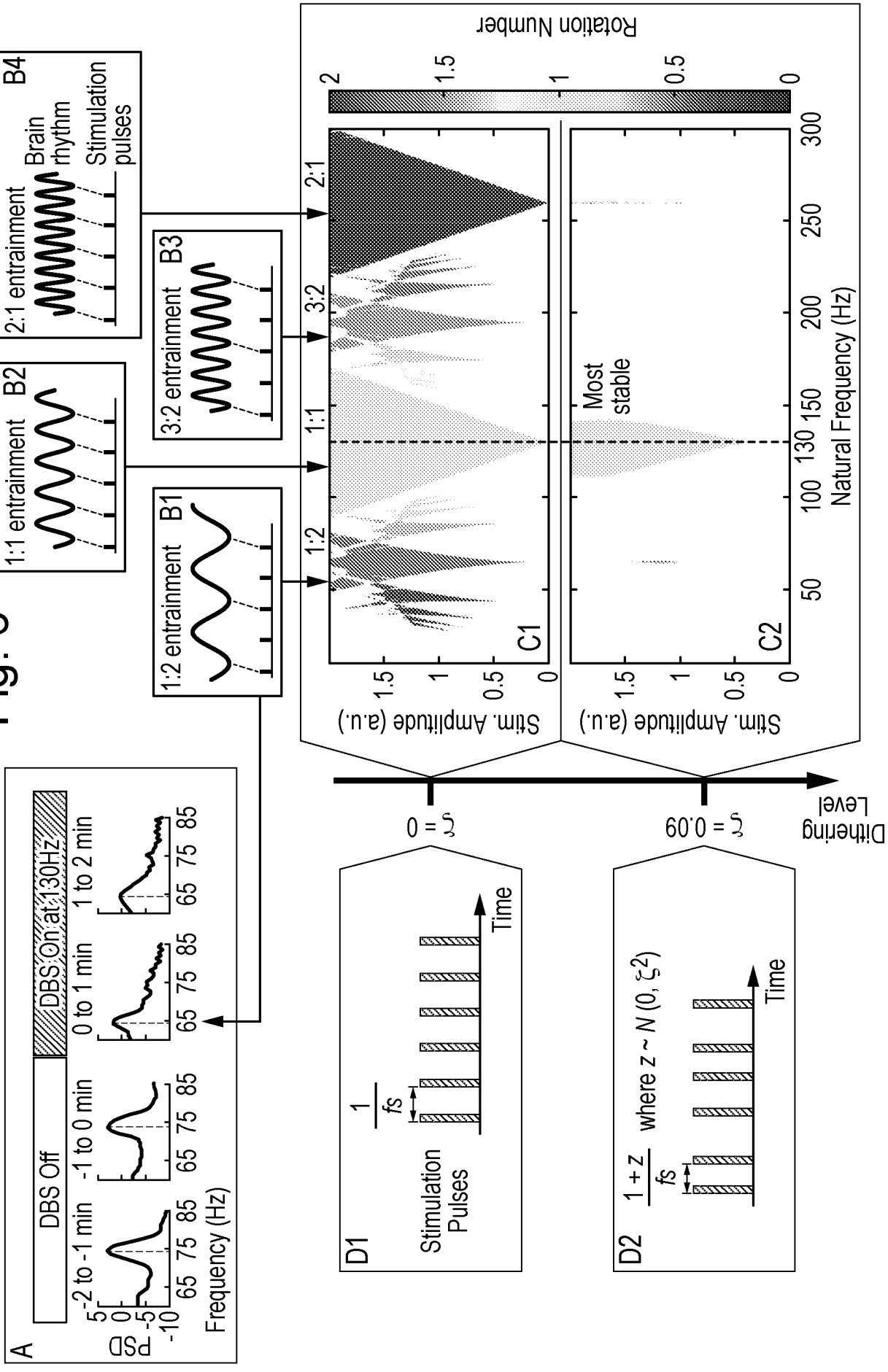
A
DBS Off
DBS On at 130Hz
-2 to -1 min
-1 to 0 min
0 to 1 min
1 to 2 min
PSD
Frequency (Hz)
B1
1:2 entrainment
B2
1:1 entrainment
B3
3:2 entrainment
B4
2:1 entrainment
Brain rhythm
Stimulation pulses
C1
C2
Stim. Amplitude (a.u.)
Most stable
Natural Frequency (Hz)
Rotation Number
Dithering Level
ζ = 0
ζ = 0.09
D1
Stimulation Pulses
Time
D2
where z ~ N (0, ζ²)
Time

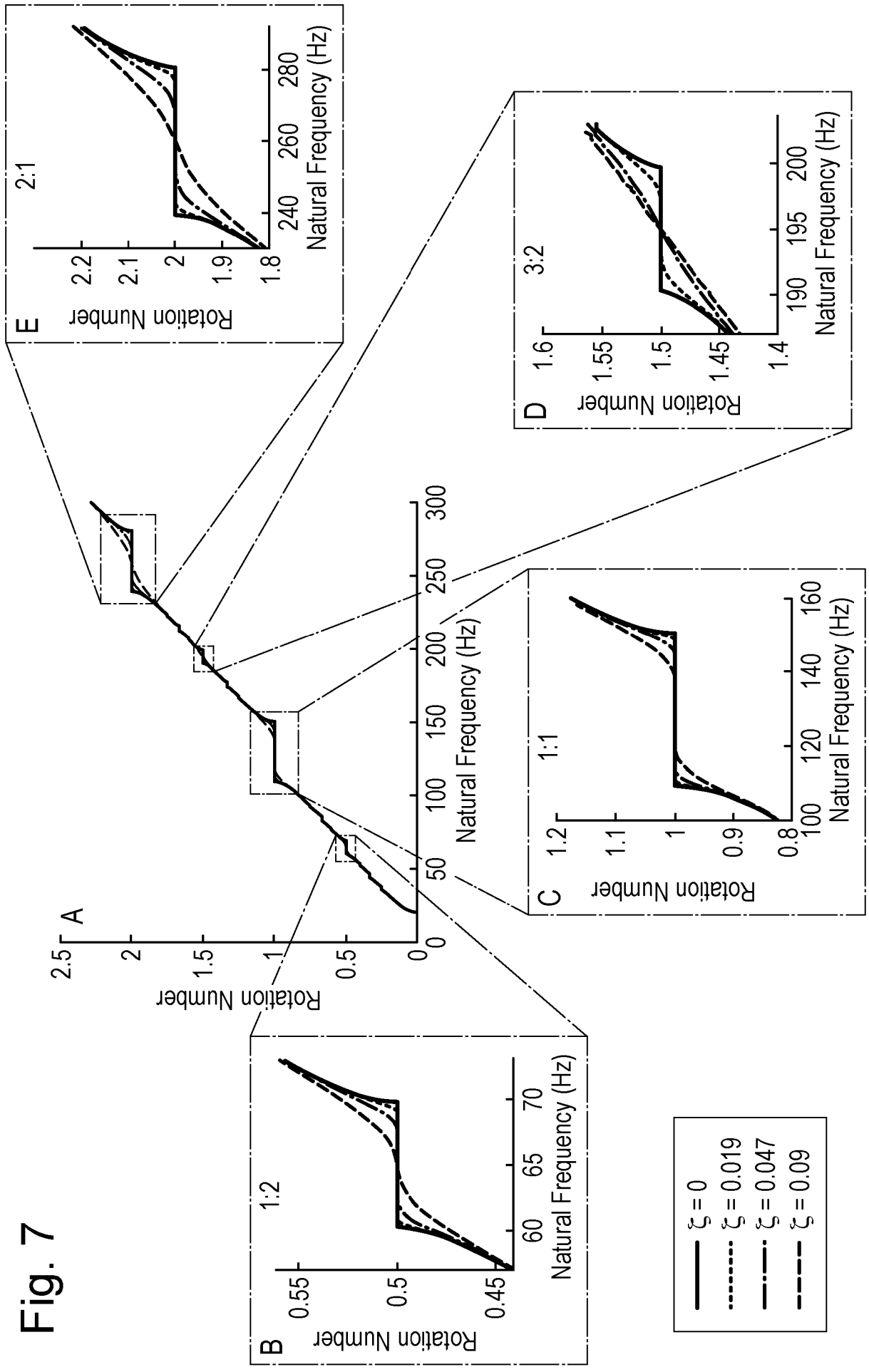
A
Rotation Number
Natural Frequency (Hz)
B
1:2
C
1:1
D
3:2
E
2:1
ζ = 0
ζ = 0.019
ζ = 0.047
ζ = 0.09

Fig. 7

Fig. 8

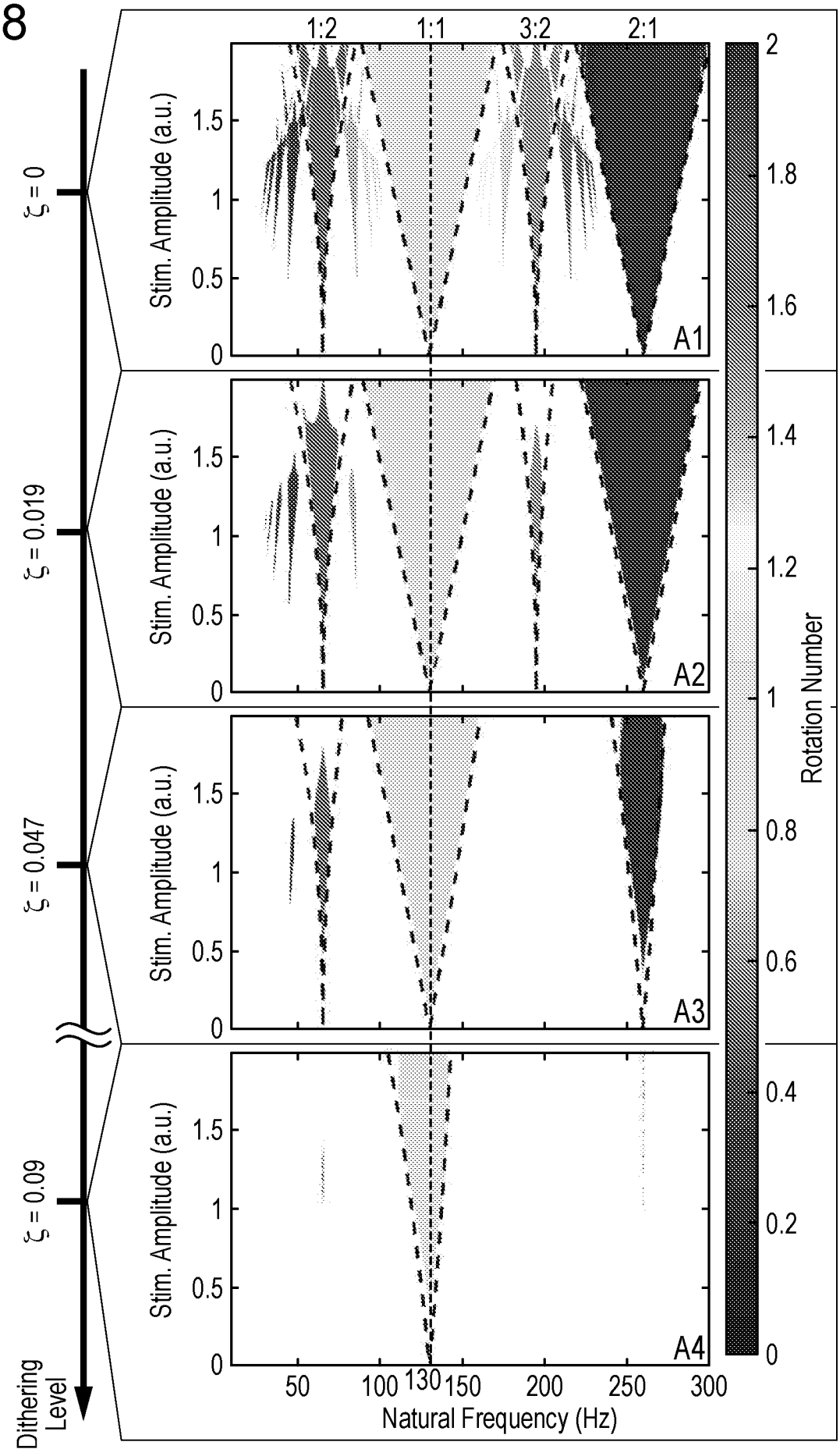
1:2
1:1
3:2
2:1
Stim. Amplitude (a.u.)
A1
A2
A3
A4
ζ = 0
ζ = 0.019
ζ = 0.047
ζ = 0.09
Dithering Level
Rotation Number
Natural Frequency (Hz)
50
100
130
150
200
250
300

# Fig. 8(Cont.)

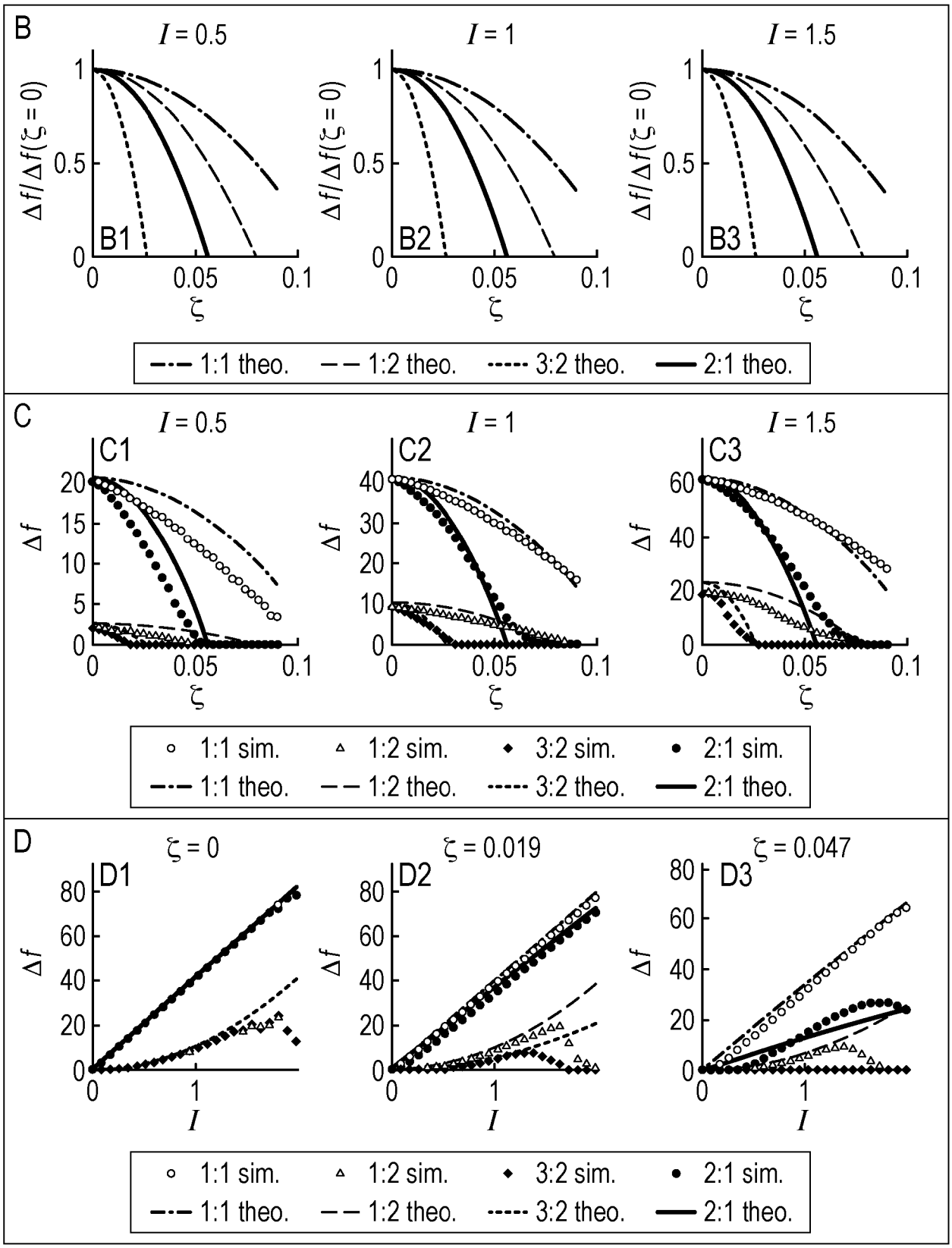
B
I = 0.5
I = 1
I = 1.5
Δf/Δf(ζ = 0)
B1
B2
B3
ζ
1:1 theo.
1:2 theo.
3:2 theo.
2:1 theo.
C
C1
C2
C3
Δf
1:1 sim.
1:2 sim.
3:2 sim.
2:1 sim.
D
ζ = 0
ζ = 0.019
ζ = 0.047
D1
D2
D3
I

Fig. 9

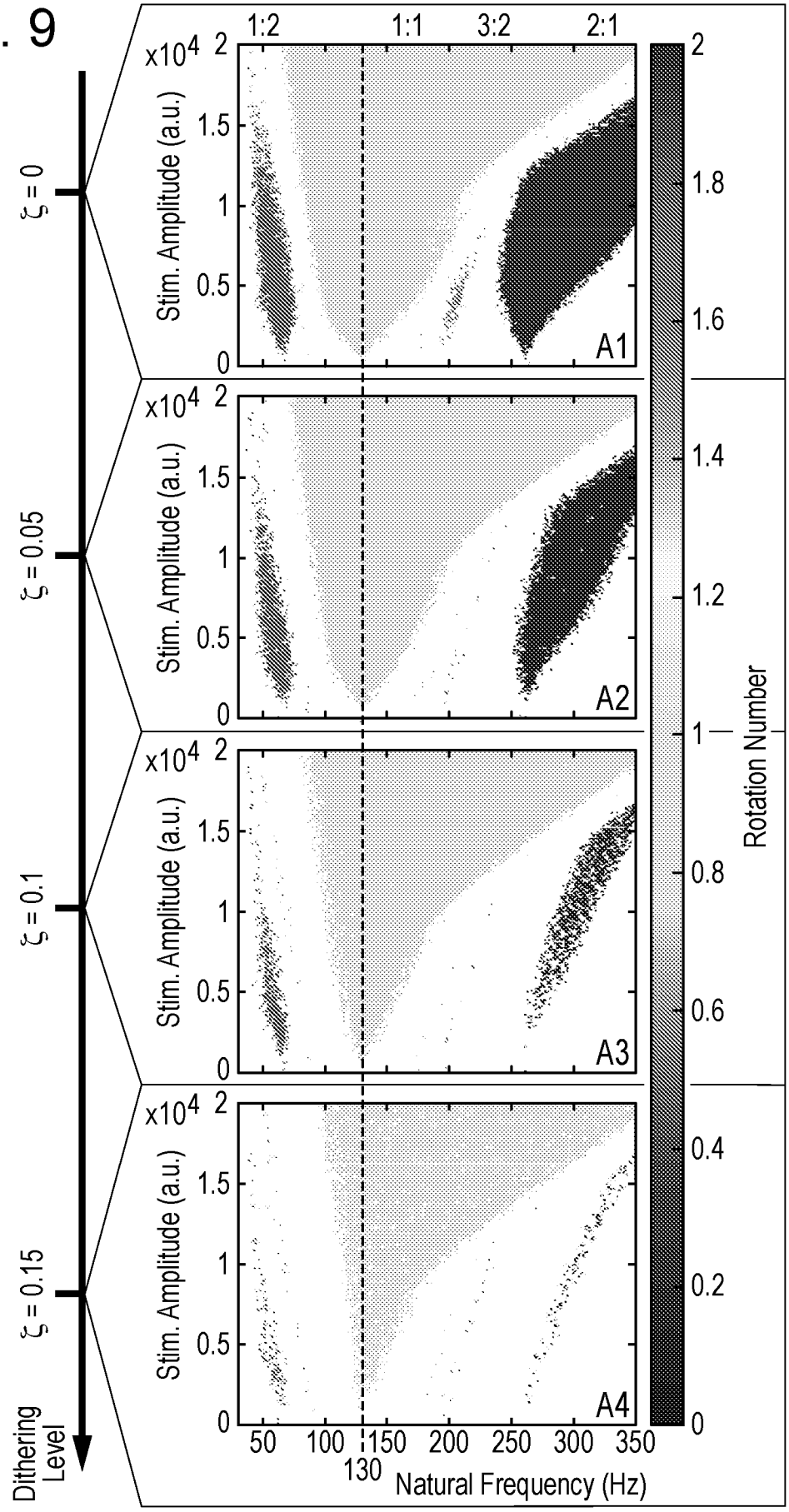
1:2
1:1
3:2
2:1
x10^4
Stim. Amplitude (a.u.)
A1
A2
A3
A4
ζ = 0
ζ = 0.05
ζ = 0.1
ζ = 0.15
Dithering Level
Rotation Number
50
100
130
150
200
250
300
350
Natural Frequency (Hz)

# Fig. 9(Cont.)

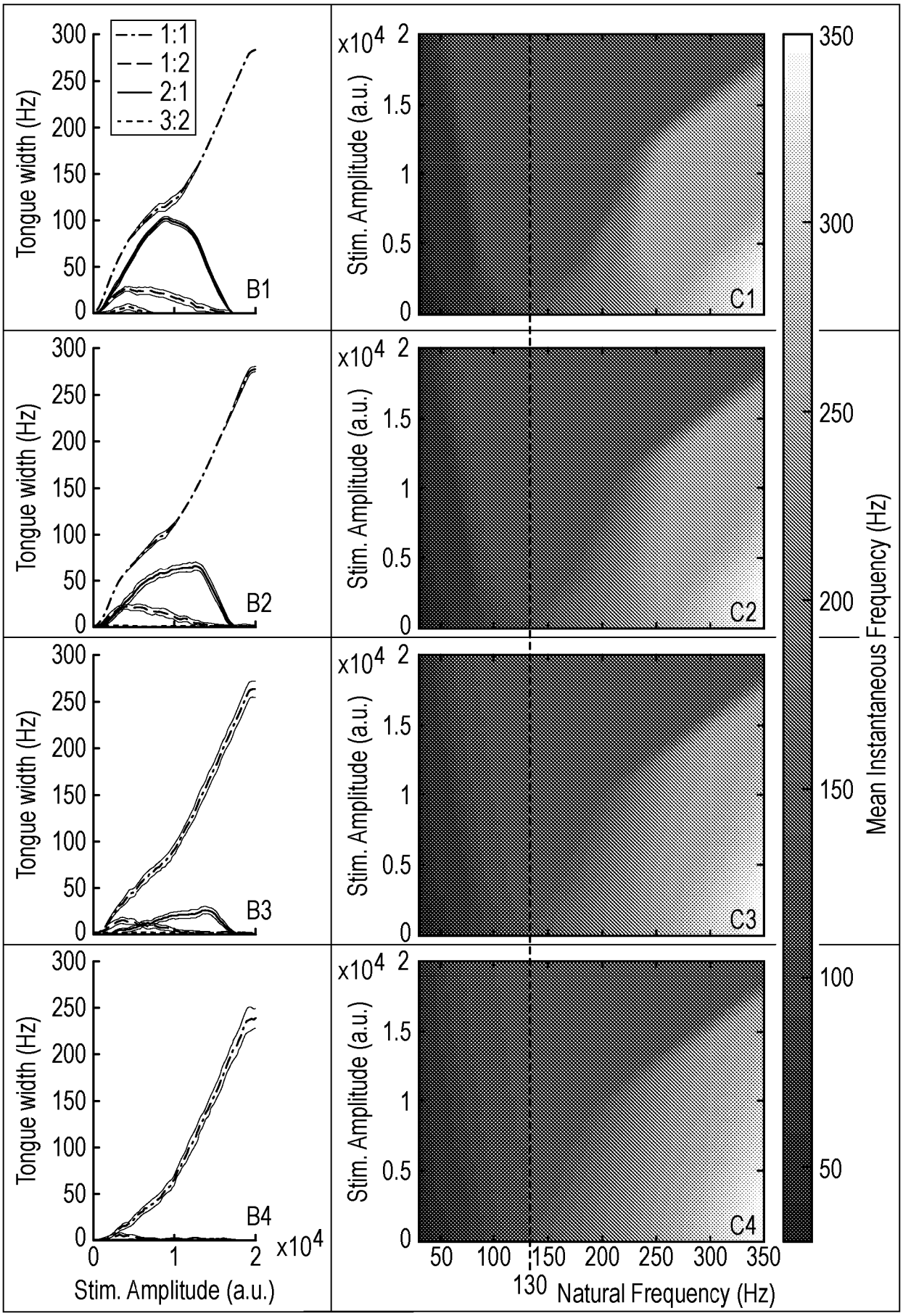
1:1
1:2
2:1
3:2
Tongue width (Hz)
Stim. Amplitude (a.u.)
x10^4
B1
B2
B3
B4
C1
C2
C3
C4
Mean Instantaneous Frequency (Hz)
Natural Frequency (Hz)
130

Fig. 10

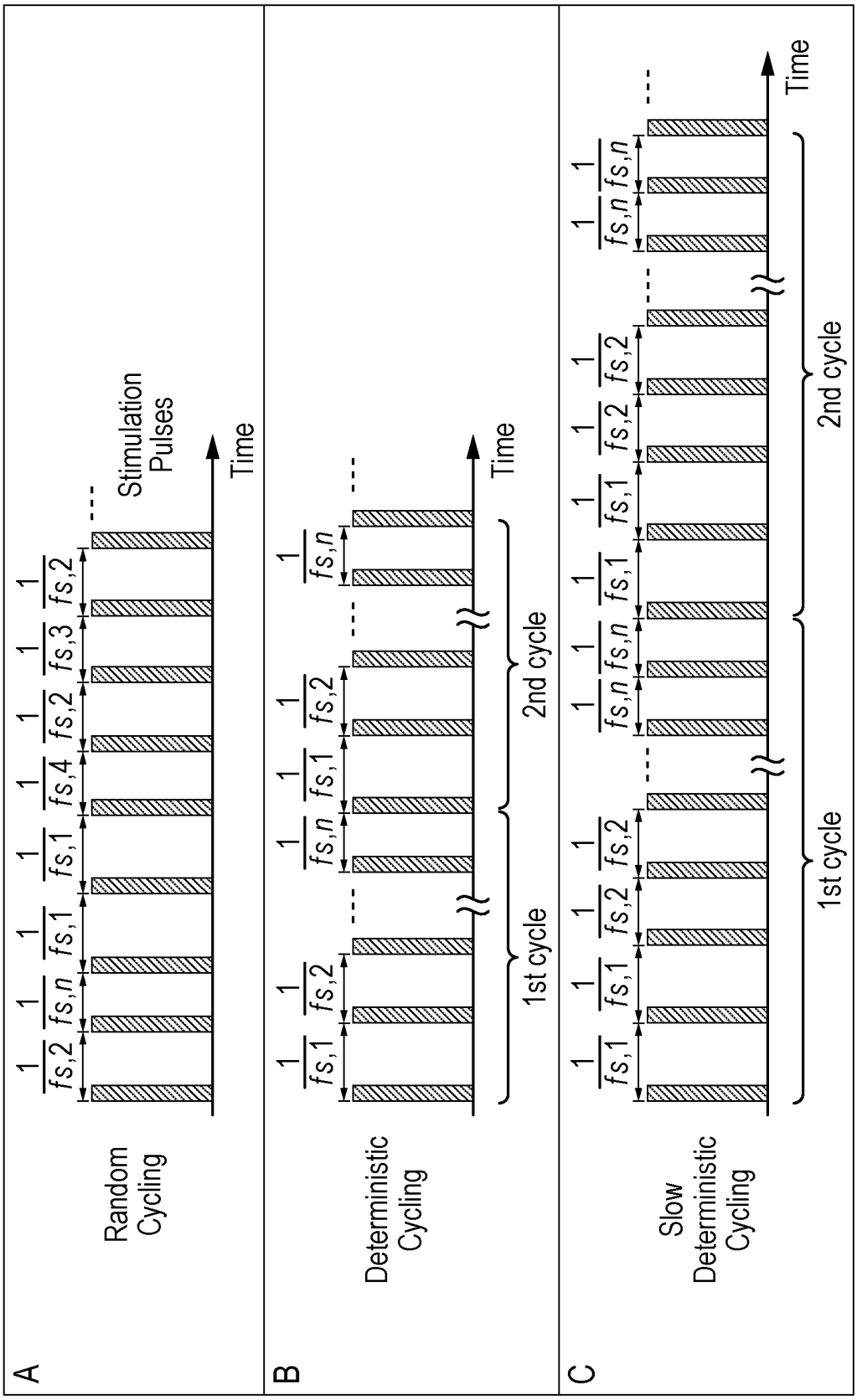
A
Random Cycling
Stimulation Pulses
Time
B
Deterministic Cycling
Time
1st cycle
2nd cycle
C
Slow Deterministic Cycling
Time
1st cycle
2nd cycle

Fig. 11

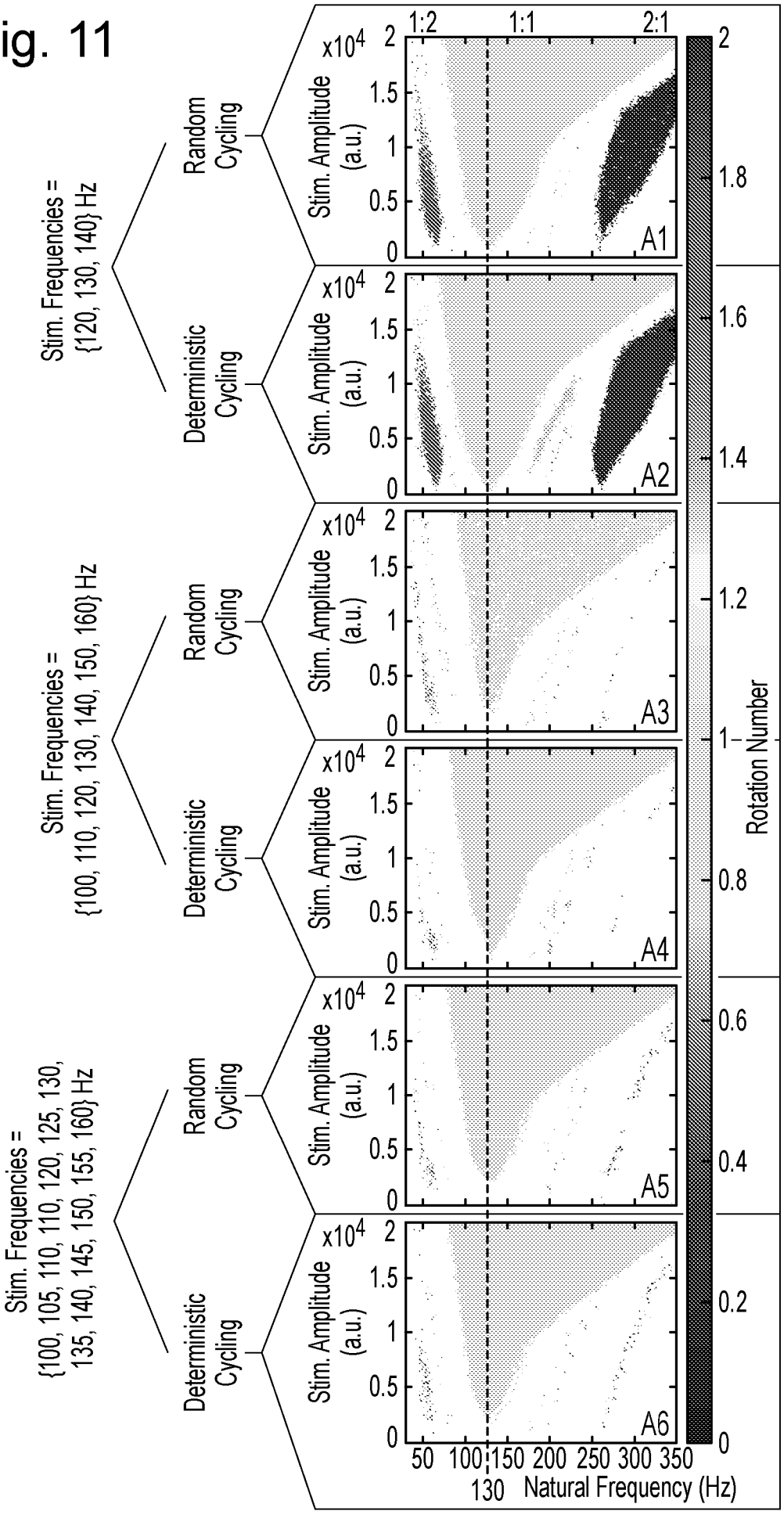
Stim. Frequencies = {120, 130, 140} Hz
Stim. Frequencies = {100, 110, 120, 130, 140, 150, 160} Hz
Stim. Frequencies = {100, 105, 110, 110, 120, 125, 130, 135, 140, 145, 150, 155, 160} Hz
Random Cycling
Deterministic Cycling
Random Cycling
Deterministic Cycling
Random Cycling
Deterministic Cycling
Stim. Amplitude (a.u.)
x10^4
2
1.5
1
0.5
0
A1
A2
A3
A4
A5
A6
1:2
1:1
2:1
50 100 130 150 200 250 300 350
Natural Frequency (Hz)
Rotation Number
2
1.8
1.6
1.4
1.2
1
0.8
0.6
0.4
0.2
0

Fig. 11 (Cont.)

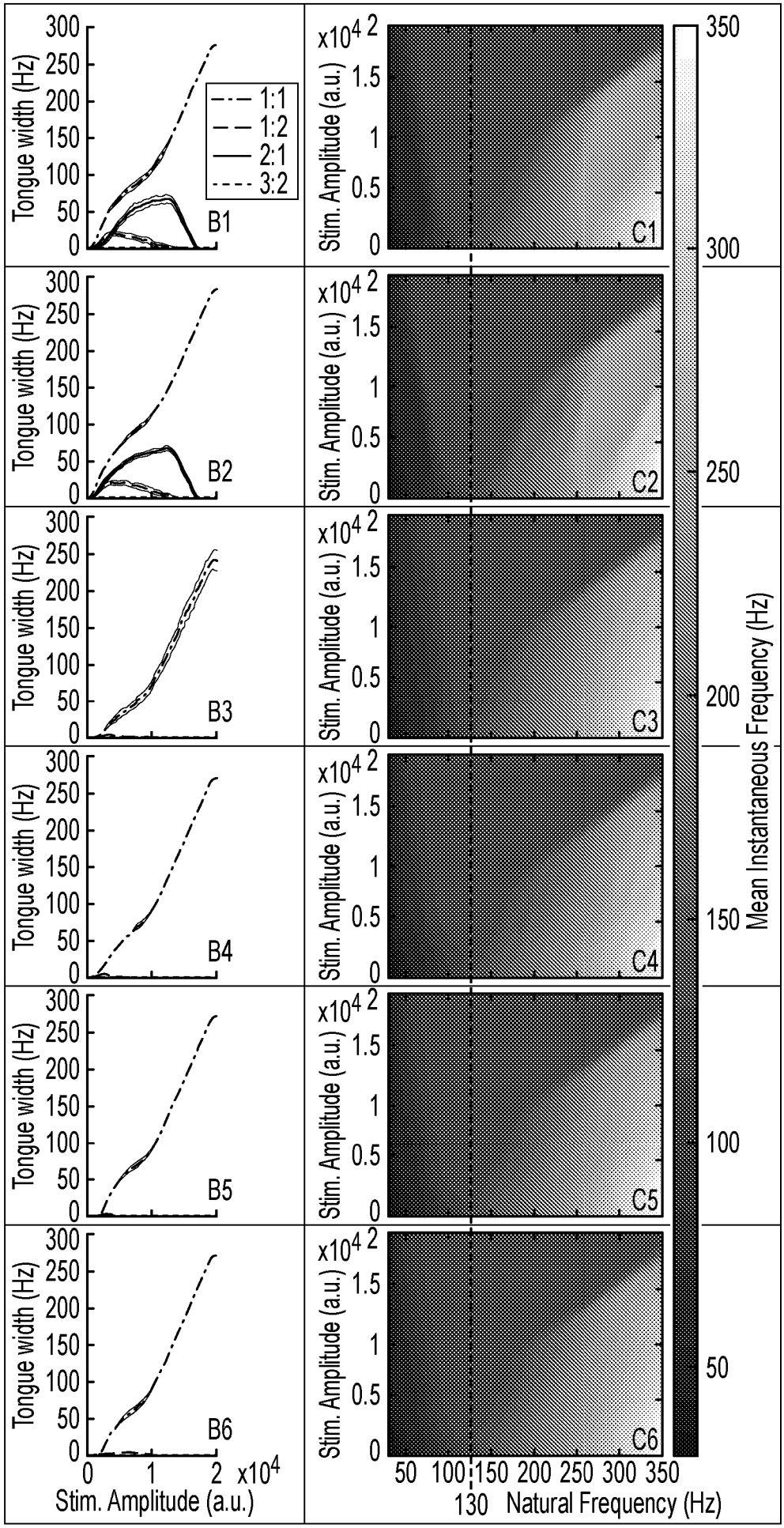
Tongue width (Hz)
300
250
200
150
100
50
0
1:1
1:2
2:1
3:2
B1
B2
B3
B4
B5
B6
0 1 2 x10^4
Stim. Amplitude (a.u.)
Stim. Amplitude (a.u.)
x10^4 2
1.5
1
0.5
0
C1
C2
C3
C4
C5
C6
50 100 150 200 250 300 350
130 Natural Frequency (Hz)
350
300
250
200
150
100
50
Mean Instantaneous Frequency (Hz)

Fig. 12

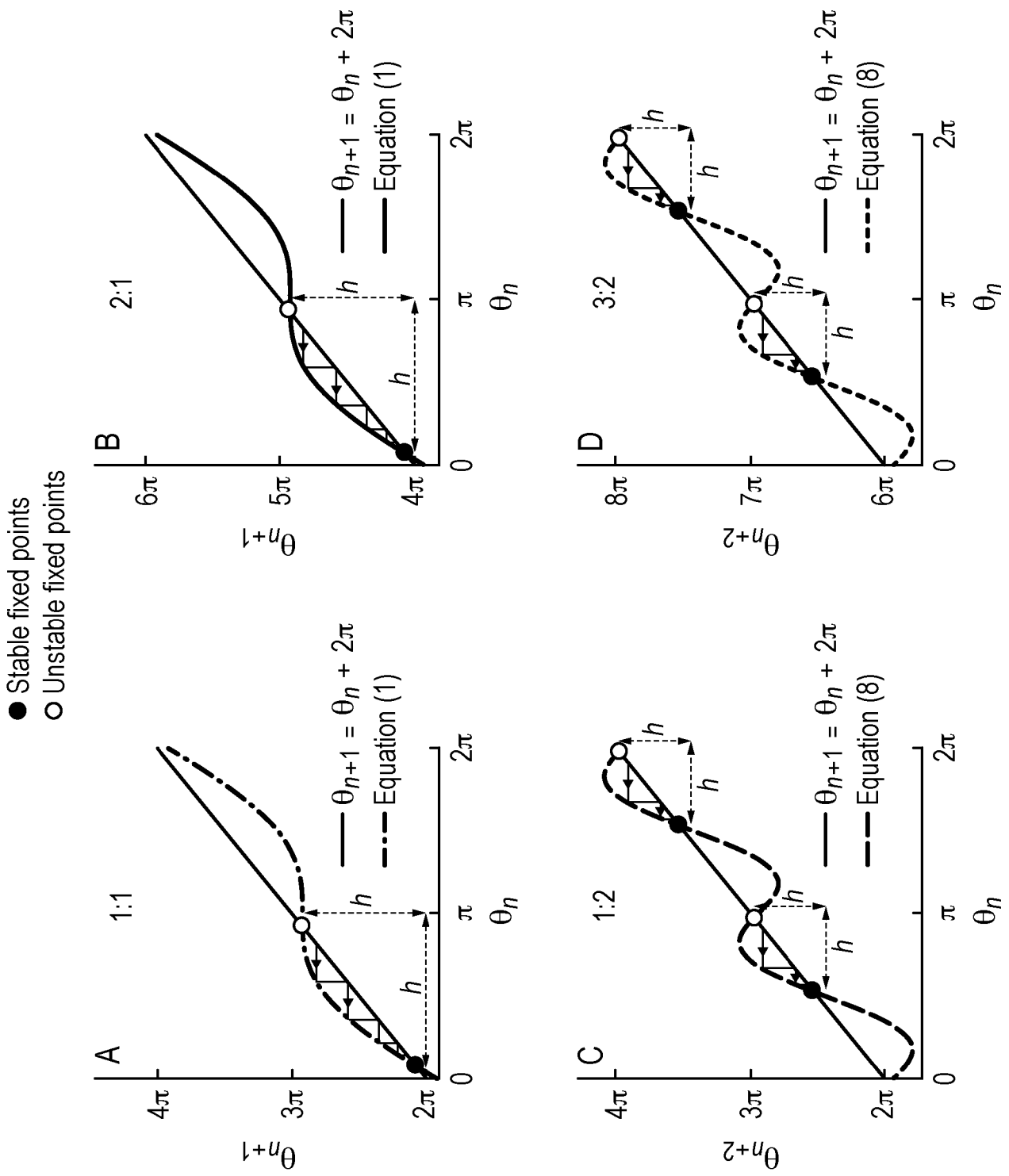
● Stable fixed points
○ Unstable fixed points
A
1:1
B
2:1
C
1:2
D
3:2
$\theta_{n+1} = \theta_n + 2\pi$
Equation (1)
Equation (8)
$\theta_{n+1}$
$\theta_{n+2}$
$\theta_n$
h
0
π
2π
3π
4π
5π
6π
7π
8π

Fig. 13

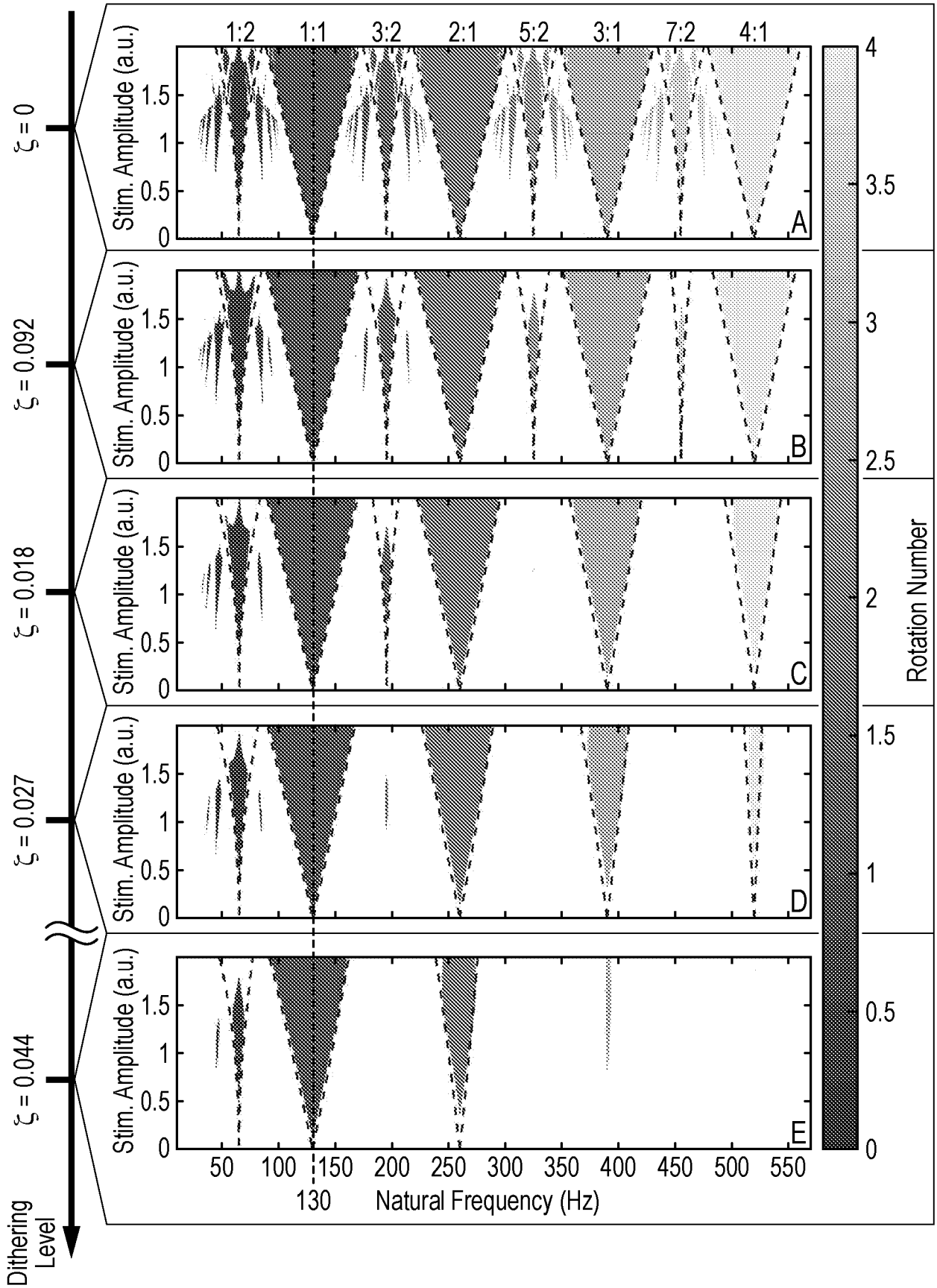
1:2
1:1
3:2
2:1
5:2
3:1
7:2
4:1
Stim. Amplitude (a.u.)
A
B
C
D
E
ζ = 0
ζ = 0.092
ζ = 0.018
ζ = 0.027
ζ = 0.044
Dithering Level
Rotation Number
4
3.5
3
2.5
2
1.5
1
0.5
0
50 100 150 200 250 300 350 400 450 500 550
130
Natural Frequency (Hz)

Fig. 14

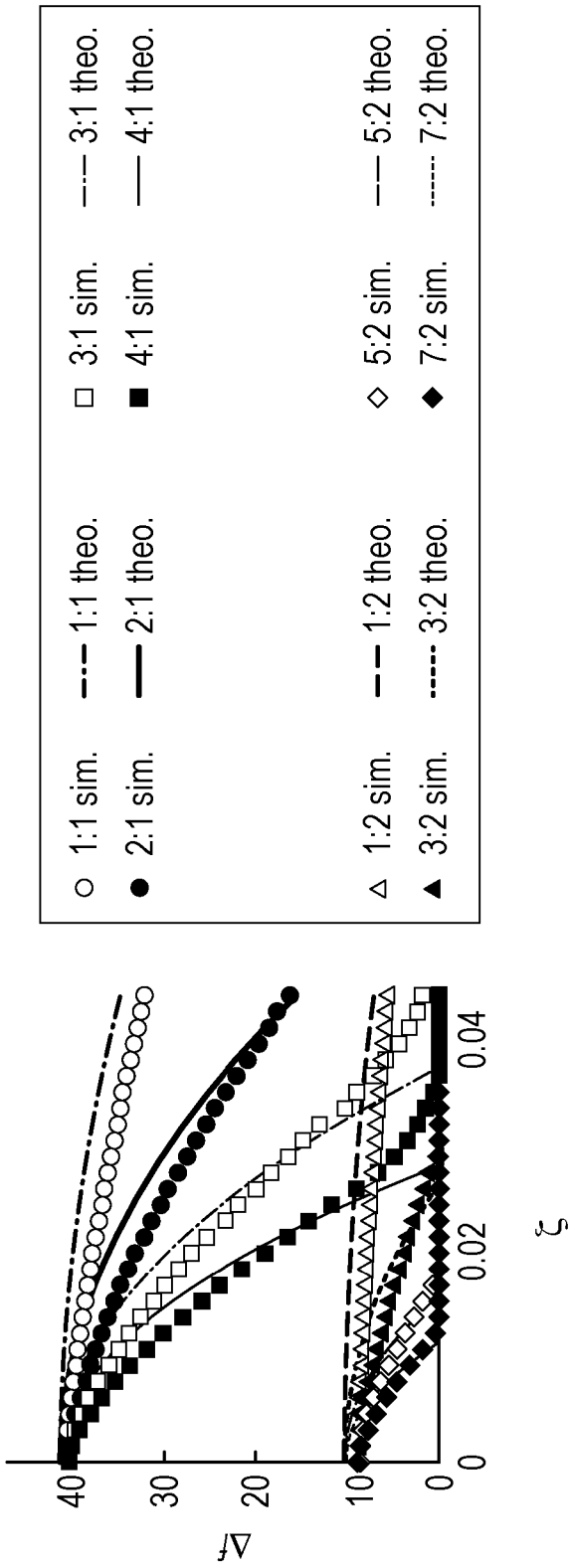
○ 1:1 sim.
1:1 theo.
□ 3:1 sim.
3:1 theo.
● 2:1 sim.
2:1 theo.
■ 4:1 sim.
4:1 theo.
△ 1:2 sim.
1:2 theo.
◇ 5:2 sim.
5:2 theo.
▲ 3:2 sim.
3:2 theo.
◆ 7:2 sim.
7:2 theo.
Δf
40
30
20
10
0
0
0.02
0.04
ζ

Fig. 15

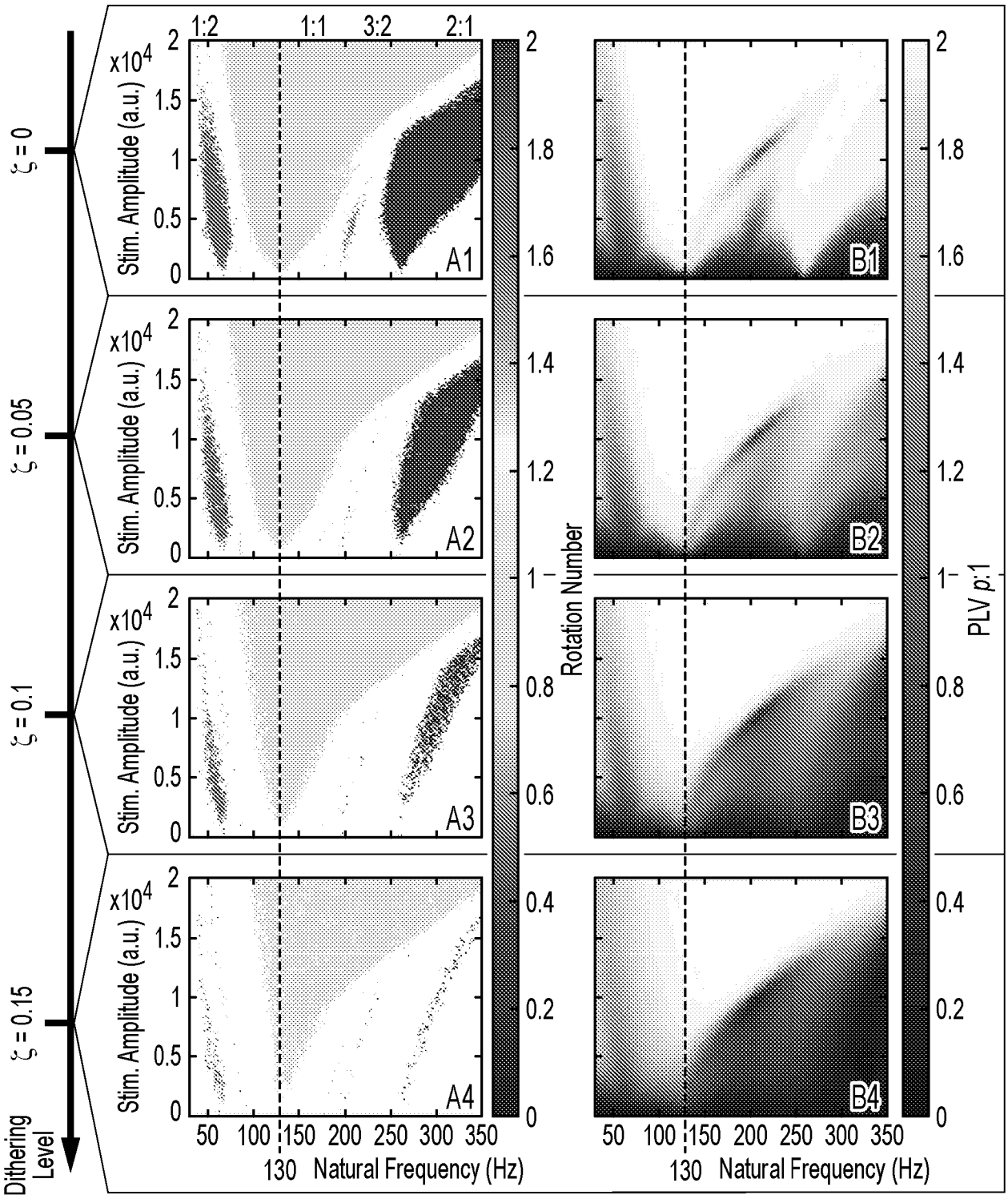
1:2
1:1
3:2
2:1
ζ = 0
ζ = 0.05
ζ = 0.1
ζ = 0.15
Dithering Level
Stim. Amplitude (a.u.)
x10^4
A1
A2
A3
A4
B1
B2
B3
B4
Rotation Number
PLV p:1
Natural Frequency (Hz)
130

# Fig. 15(Cont.)

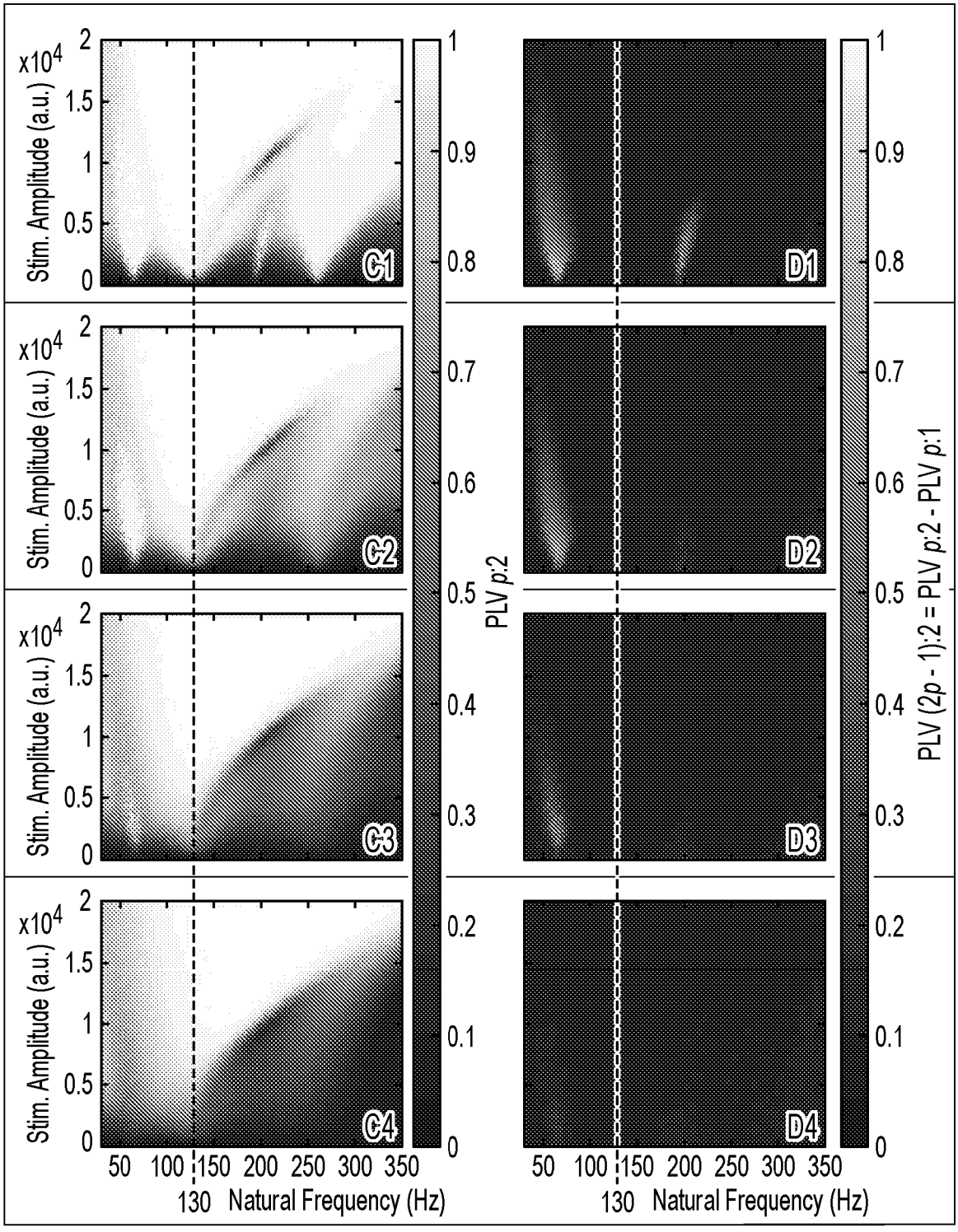
x10^4
Stim. Amplitude (a.u.)
2
1.5
1
0.5
0
C1
C2
C3
C4
D1
D2
D3
D4
1
0.9
0.8
0.7
0.6
0.5
0.4
0.3
0.2
0.1
0
PLV p:2
PLV (2p - 1):2 = PLV p:2 - PLV p:1
50 100 130 150 200 250 300 350
Natural Frequency (Hz)

Fig. 16

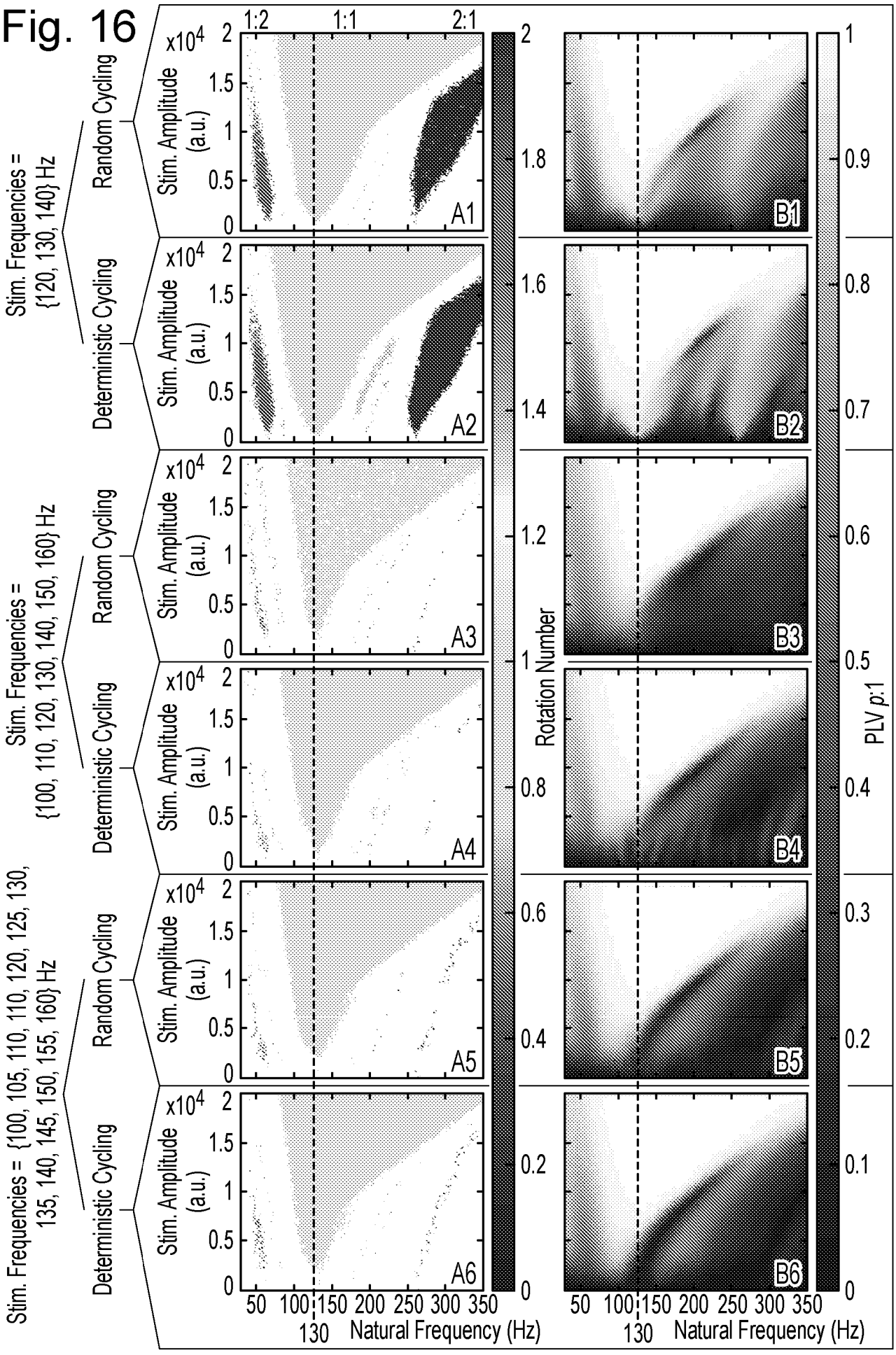
Stim. Frequencies = {100, 105, 110, 110, 120, 125, 130, 135, 140, 145, 150, 155, 160} Hz
Stim. Frequencies = {100, 110, 120, 130, 140, 150, 160} Hz
Stim. Frequencies = {120, 130, 140} Hz
Deterministic Cycling
Random Cycling
Stim. Amplitude (a.u.)
x10^4
1:2
1:1
2:1
A1
A2
A3
A4
A5
A6
B1
B2
B3
B4
B5
B6
Rotation Number
PLV p:1
50 100 130 150 200 250 300 350
Natural Frequency (Hz)

Fig. 16 (Cont.)

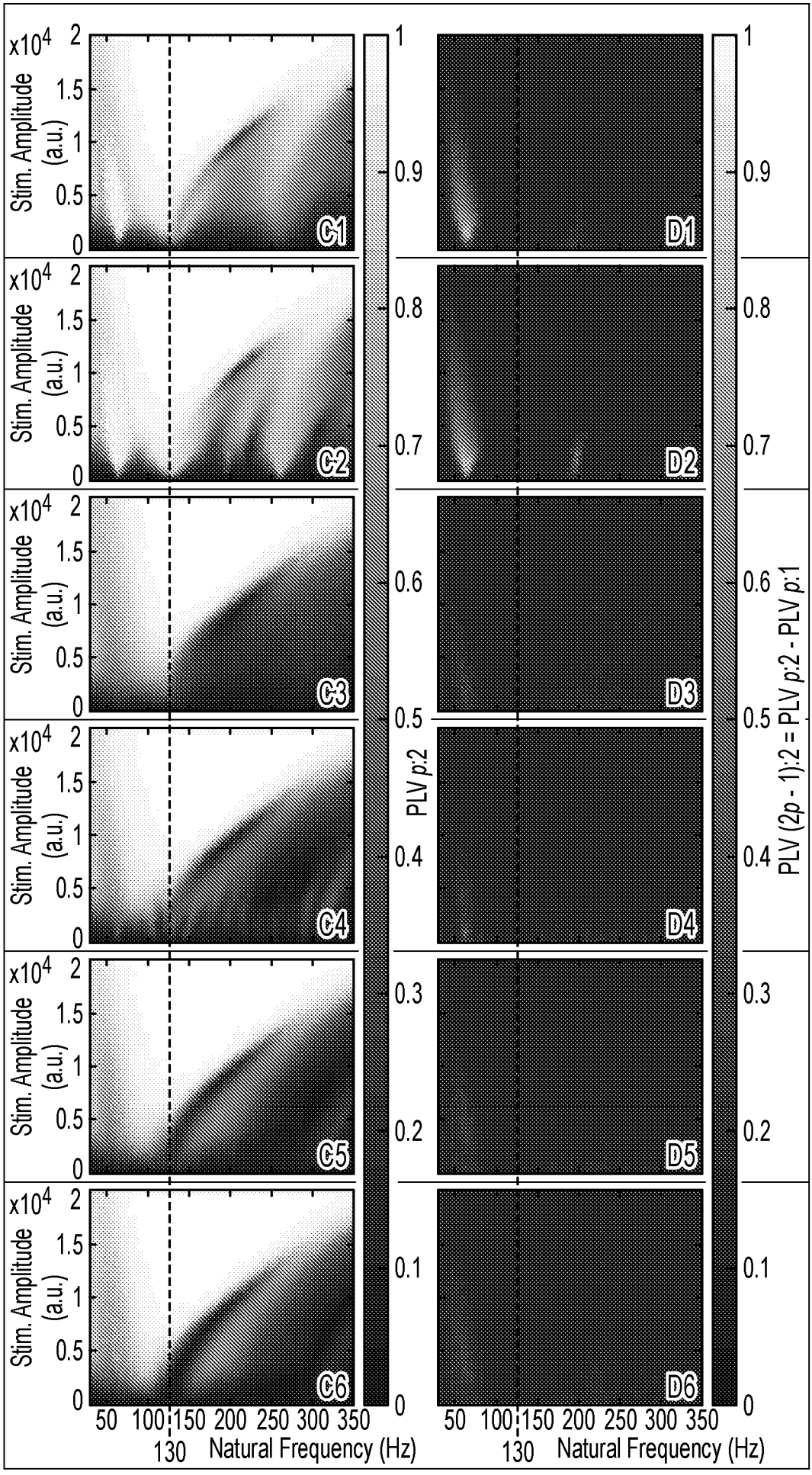
C1
C2
C3
C4
C5
C6
D1
D2
D3
D4
D5
D6
Stim. Amplitude (a.u.)
x10^4
0
0.5
1
1.5
2
50 100 150 200 250 300 350
130
Natural Frequency (Hz)
PLV p:2
PLV (2p - 1):2 = PLV p:2 - PLV p:1
0
0.1
0.2
0.3
0.4
0.5
0.6
0.7
0.8
0.9
1

Fig. 17

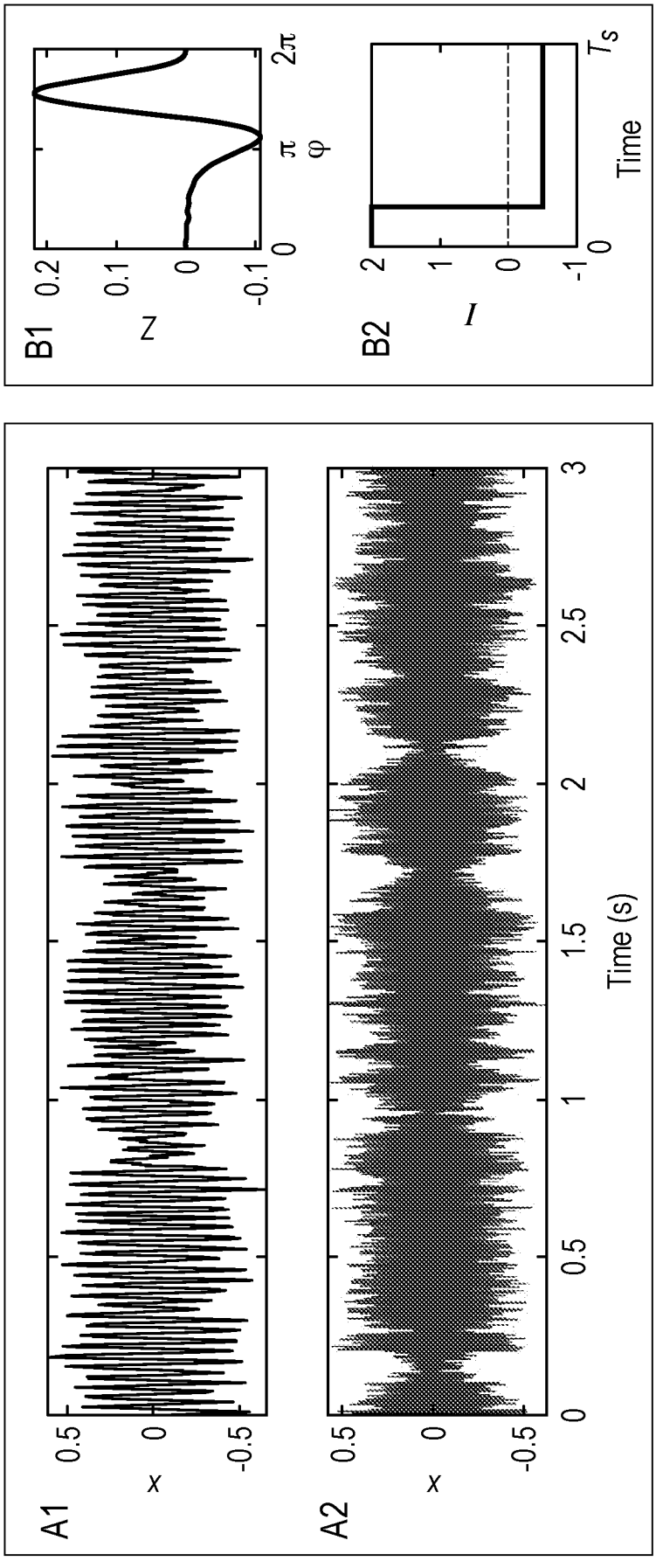
B1
0.2
0.1
0
-0.1
Z
0
π
2π
φ
B2
2
1
0
-1
I
0
Time
$T_s$
A1
0.5
0
-0.5
x
A2
0.5
0
-0.5
x
0
0.5
1
1.5
2
2.5
3
Time (s)

# INTERNATIONAL SEARCH REPORT

International application No
PCT/GB2023/051670

**A. CLASSIFICATION OF SUBJECT MATTER**

INV. A61N1/36

ADD. A61N1/02 A61B5/24 A61N1/05

According to International Patent Classification (IPC) or to both national classification and IPC

**B. FIELDS SEARCHED**

Minimum documentation searched (classification system followed by classification symbols)

A61N A61B

Documentation searched other than minimum documentation to the extent that such documents are included in the fields searched

Electronic data base consulted during the international search (name of data base and, where practicable, search terms used)

EPO-Internal

**C. DOCUMENTS CONSIDERED TO BE RELEVANT**

| Category* | Citation of document, with indication, where appropriate, of the relevant passages | Relevant to claim No. |
|---|---|---|
| A | US 2006/030897 A1 (GILMER JAMES R [US] ET AL) 9 February 2006 (2006-02-09) paragraphs [0019] - [0020], [0026] - [0027] | 1-25 |
| A | WO 2021/250398 A1 (UNIV OXFORD INNOVATION LTD [GB]) 16 December 2021 (2021-12-16) page 2, line 22 - page 3, line 13 | 1-25 |

-/--

[X] Further documents are listed in the continuation of Box C.

[X] See patent family annex.

* Special categories of cited documents :

"A" document defining the general state of the art which is not considered to be of particular relevance

"E" earlier application or patent but published on or after the international filing date

"L" document which may throw doubts on priority claim(s) or which is cited to establish the publication date of another citation or other special reason (as specified)

"O" document referring to an oral disclosure, use, exhibition or other means

"P" document published prior to the international filing date but later than the priority date claimed

"T" later document published after the international filing date or priority date and not in conflict with the application but cited to understand the principle or theory underlying the invention

"X" document of particular relevance;; the claimed invention cannot be considered novel or cannot be considered to involve an inventive step when the document is taken alone

"Y" document of particular relevance;; the claimed invention cannot be considered to involve an inventive step when the document is combined with one or more other such documents, such combination being obvious to a person skilled in the art

"&" document member of the same patent family

| Date of the actual completion of the international search | Date of mailing of the international search report |
|---|---|
| 12 September 2023 | 20/09/2023 |

| Name and mailing address of the ISA/ | Authorized officer |
|---|---|
| European Patent Office, P.B. 5818 Patentlaan 2<br>NL - 2280 HV Rijswijk<br>Tel. (+31-70) 340-2040,<br>Fax: (+31-70) 340-3016 | Rogala, Tomasz |

1

# INTERNATIONAL SEARCH REPORT

International application No
PCT/GB2023/051670

C(Continuation). DOCUMENTS CONSIDERED TO BE RELEVANT

| Category* | Citation of document, with indication, where appropriate, of the relevant passages | Relevant to claim No. |
|---|---|---|
| A | NEGAHBANI EHSAN ET AL: "Targeting alpha-band oscillations in a cortical model with amplitude-modulated high-frequency transcranial electric stimulation", NEUROIMAGE, ELSEVIER, AMSTERDAM, NL, vol. 173, 7 February 2018 (2018-02-07), pages 3-12, XP085382214, ISSN: 1053-8119, DOI: 10.1016/J.NEUROIMAGE.2018.02.005 section "Modelling of cortical oscillations"; page 5, left-hand column<br>----- | 1-25 |
| A | US 2020/155852 A1 (DE RIDDER DIRK [NZ]) 21 May 2020 (2020-05-21) paragraphs [0072] - [0074]; figure 4<br>----- | 1-25 |

# INTERNATIONAL SEARCH REPORT

International application No.
PCT/GB2023/051670

**Box No. II Observations where certain claims were found unsearchable (Continuation of item 2 of first sheet)**

This international search report has not been established in respect of certain claims under Article 17(2)(a) for the following reasons:

1. [X] Claims Nos.: 26-32
because they relate to subject matter not required to be searched by this Authority, namely:
see FURTHER INFORMATION sheet PCT/ISA/210

2. [ ] Claims Nos.:
because they relate to parts of the international application that do not comply with the prescribed requirements to such an extent that no meaningful international search can be carried out, specifically:

3. [ ] Claims Nos.:
because they are dependent claims and are not drafted in accordance with the second and third sentences of Rule 6.4(a).

**Box No. III Observations where unity of invention is lacking (Continuation of item 3 of first sheet)**

This International Searching Authority found multiple inventions in this international application, as follows:

1. [ ] As all required additional search fees were timely paid by the applicant, this international search report covers all searchable claims.

2. [ ] As all searchable claims could be searched without effort justifying an additional fees, this Authority did not invite payment of additional fees.

3. [ ] As only some of the required additional search fees were timely paid by the applicant, this international search report covers only those claims for which fees were paid, specifically claims Nos.:

4. [ ] No required additional search fees were timely paid by the applicant. Consequently, this international search report is restricted to the invention first mentioned in the claims;; it is covered by claims Nos.:

**Remark on Protest**

[ ] The additional search fees were accompanied by the applicant's protest and, where applicable, the payment of a protest fee.

[ ] The additional search fees were accompanied by the applicant's protest but the applicable protest fee was not paid within the time limit specified in the invitation.

[ ] No protest accompanied the payment of additional search fees.

FURTHER INFORMATION CONTINUED FROM PCT/ISA/ 210

Continuation of Box II.1

Claims Nos.: 26-32

The method defined in claim 26 and claims 27-32 dependent thereon relates to therapeutical treatment of the human or animal body. This is due to the fact that a method of "operating" a neural stimulation device at least implicitly encompasses also its intended use, i.e. the neural stimulation itself, which may have (and in view of the description is actually intended to have) a therapeutic effect. Thus, claims 26-32 are covered by the provisions of Article 17(2)(a)(i) PCT and Rule 39.1 (iv) PCT, i.e. the International Search Authority cannot be required to perform the search on their subject-matter. Moreover, according to Article 34(4)(a)(i) PCT and Rule 67.1 (iv) PCT, no examination is required to be carried out on these claims.

# INTERNATIONAL SEARCH REPORT

Information on patent family members

International application No
PCT/GB2023/051670

| Patent document cited in search report | Publication date | Patent family member(s) | Publication date |
|---|---|---|---|
| US 2006030897 A1 | 09-02-2006 | NONE | |
| WO 2021250398 A1 | 16-12-2021 | EP 4164733 A1 | 19-04-2023 |
| | | US 2023271012 A1 | 31-08-2023 |
| | | WO 2021250398 A1 | 16-12-2021 |
| US 2020155852 A1 | 21-05-2020 | AU 2015313928 A1 | 23-03-2017 |
| | | AU 2020201736 A1 | 26-03-2020 |
| | | AU 2021225198 A1 | 30-09-2021 |
| | | EP 3191178 A2 | 19-07-2017 |
| | | US 2016074663 A1 | 17-03-2016 |
| | | US 2019015666 A1 | 17-01-2019 |
| | | US 2020155852 A1 | 21-05-2020 |
| | | WO 2016038464 A2 | 17-03-2016 |